

# 8 Thermal Properties

---

This chapter considers composites for thermal applications, including the basic principles related to the thermal behavior of materials. The applications include thermal conduction, heat dissipation, thermal insulation, heat retention, heat storage, rewritable optical discs, and shape-memory actuation.

## 8.1 Thermal Expansion

Upon heating, the length of a solid typically increases. Upon cooling, its length typically decreases. This phenomenon is known as thermal expansion.

The coefficient of thermal expansion (CTE, also abbreviated to  $\alpha$ ) is defined as

$$\alpha = (1/L_0)(\Delta L/\Delta T), \quad (8.1)$$

where  $L_0$  is the original length and  $L$  is the length at temperature  $T$ . In other words,  $\alpha$  is the fractional change in length per unit change in temperature (i.e., strain per unit change in temperature). Equation 8.1 can be rewritten as

$$\Delta L/L_0 = \alpha \Delta T. \quad (8.2)$$

Thermal expansion is reversible, so thermal contraction occurs upon cooling, and the extent of thermal contraction is also governed by  $\alpha$ .

The change in dimensions that occurs upon changing the temperature may be undesirable when the dimensional change results in thermal stress; i.e., internal stress associated with the fact that the dimensions are not the same as those the component should have when it is not constrained. An example concerns a joint between two components that exhibit different thermal expansion coefficients. The joint is created at a given temperature. Subsequent to the bonding, the joint is heated or cooled. Upon heating or cooling, the bonding constrains the dimensions of both components, thus causing both components to be unable to attain the dimensions that they would do if they were not bonded. When the thermal stress is too high, deformation such as warpage may occur. Debonding can even occur. If thermal cycling occurs, the thermal stress is cycled, thus resulting in thermal fatigue when the number of thermal cycles is sufficiently high.

Thermal expansion can be advantageously used to obtain a tight fit between two components. For example, a pipe (preferably one with a rather high coefficient of

thermal expansion) is cooled and then, in the cold state, inserted into a larger pipe. Upon subsequent warming of the inner pipe, thermal expansion causes a tight fit between the two pipes.

The energy associated with a bond depends on the bond distance (i.e., the bond length), as shown in Fig. 8.1a. The energy is lowest at the equilibrium bond distance. The curve of energy vs. bond distance takes the shape of a trough that is asymmetric. The higher the temperature, the higher is the energy, and the average bond distance (the midpoint of the horizontal line cutting across the energy trough) increases. Thermal expansion stems from the increasing amplitude of thermal vibrations with increasing temperature and the greater ease of outward vibration (bond lengthening) than inward vibration (bond shortening), reflecting the asymmetry in the energy versus bond length curve. This asymmetry causes the distance QR to be greater than the distance QP in Fig. 8.1b, so that the outward vibration travels a greater distance than the inward vibration at a given temperature. The depth of the energy trough below the energy of zero is the bond energy. At the energy minimum, the bond length is the equilibrium value. A weaker bond has a lower bond energy and corresponds to greater asymmetry in the energy trough. Greater asymmetry means a higher value of the CTE. Hence, weaker bonding tends to give a higher CTE.

Table 8.1 shows that the CTE tends to be high for polymers, medium for metals, and low for ceramics. This reflects the weak intermolecular bonding in polymers,

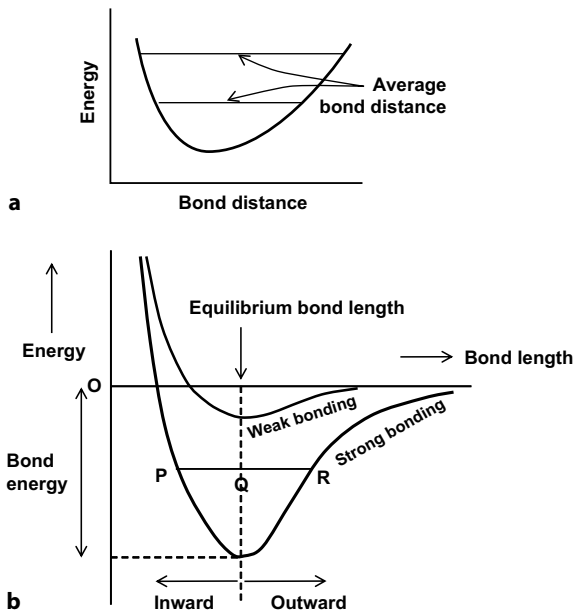


**Figure 8.1.** Dependence of the energy between two atoms on the distance between the atoms. **a** The average bond distance, which occurs at the midpoint of the horizontal line across the energy trough at a given energy, increases with increasing energy. **b** Comparison of a solid with strong bonding and one with weak bonding. The equilibrium bond length occurs at the minimum energy

**Table 8.1.** Coefficients of thermal expansion (CTEs) of various materials at 20°C

Material	CTE ( $10^{-6}/\text{K}$ )
Rubber <sup>a</sup>	77
Polyvinyl chloride <sup>a</sup>	52
Lead <sup>b</sup>	29
Magnesium <sup>b</sup>	26
Aluminum <sup>b</sup>	23
Brass <sup>b</sup>	19
Silver <sup>b</sup>	18
Stainless steel <sup>b</sup>	17.3
Copper <sup>b</sup>	17
Gold <sup>b</sup>	14
Nickel <sup>b</sup>	13
Steel <sup>b</sup>	11.0–13.0
Iron <sup>b</sup>	11.1
Carbon steel <sup>b</sup>	10.8
Platinum <sup>b</sup>	9
Tungsten <sup>b</sup>	4.5
Invar (Fe-Ni36) <sup>b</sup>	1.2
Concrete <sup>c</sup>	12
Glass <sup>c</sup>	8.5
Gallium arsenide <sup>c</sup>	5.8
Indium phosphide <sup>c</sup>	4.6
Glass, borosilicate <sup>c</sup>	3.3
Quartz (fused) <sup>c</sup>	0.59
Silicon	3
Diamond	1

<sup>a</sup> Polymer; <sup>b</sup> metal; <sup>c</sup> ceramic

the moderately strong metallic bonding in metals, and the strong ionic/covalent bonding in ceramics. Silicon and diamond are not ceramics, but their CTE values are low because they are covalent network solids. Because stronger bonding tends to give a higher melting temperature, a lower CTE tends to correlate with a higher melting temperature. This is why tungsten, with a very high melting temperature of 3,410°C, has a low CTE of  $4.5 \times 10^{-6}/\text{K}$ . In contrast, magnesium, with a low melting temperature of 660°C, has a high CTE of 23. Invar (Fe-Ni36) has an exceptionally low CTE among metals because of its magnetic character (due to the iron part of the alloy) and the effect of the magnetic moment on the volume. Among ceramics, quartz has a particularly low CTE due to its three-dimensional network of covalent/ionic bonding. Glass has a higher CTE than quartz due to its lower degree of networking.

The CTE of a composite can be calculated from those of its components. When the components are placed in series, as illustrated in Fig. 8.2a, the change in length  $\Delta L_c$  of the composite is given by the sum of the changes in the lengths of the components:

$$\Delta L_c = \Delta L_1 + \Delta L_2 , \quad (8.3)$$

where  $\Delta L_1$  and  $\Delta L_2$  are the changes in the lengths of the components. Only two components are shown in the summation in Eq. 8.3 for the sake of simplicity. Dividing by the original length  $L_{c0}$  of the composite gives

$$\Delta L_c/L_{c0} = \Delta L_1/L_{c0} + \Delta L_2/L_{c0} = \nu_1 \Delta L_1/L_{10} + \nu_2 \Delta L_2/L_{20} , \tag{8.4}$$

where  $L_{10}$  and  $L_{20}$  are, respectively, the original lengths of component 1 (all of the strips of component 1 together) and component 2 (all the strips of component 2 together), and  $\nu_1$  and  $\nu_2$  are the volume fractions of components 1 and 2, respectively. In Eq. 8.4, the relations

$$L_{10} = \nu_1 L_{c0} , \tag{8.5}$$

and

$$L_{20} = \nu_2 L_{c0} \tag{8.6}$$

have been used. Using Eq. 8.2, Eq. 8.4 becomes

$$\alpha_c \Delta T = \nu_1 \alpha_1 \Delta T + \nu_2 \alpha_2 \Delta T , \tag{8.7}$$

where  $\alpha_c$  is the CTE of the composite and  $\alpha_1$  and  $\alpha_2$  are the CTEs of components 1 and 2, respectively. Division by  $\Delta T$  gives

$$\alpha_c = \nu_1 \alpha_1 + \nu_2 \alpha_2 . \tag{8.8}$$

Equation 8.8 is the rule of mixtures expression for the CTE of the composite in the case of the series configuration shown in Fig. 8.2a.

For the parallel configuration of Fig. 8.2b, when the component strips are perfectly bonded to one another, the two components are constrained so that their lengths are the same at any temperature. This constraint causes each component

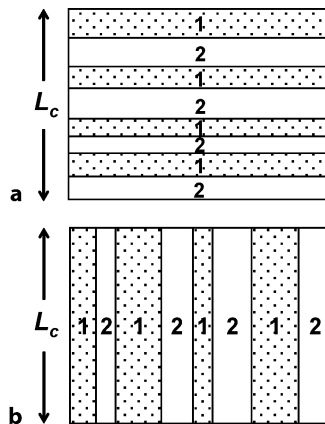


**Figure 8.2.** Calculation of the CTE of a composite with two components, labeled 1 and 2. **a** Series configuration, **b** parallel configuration

to be unable to change its length by the amount dictated by its CTE (Eq. 8.2). As a result, each component experiences a thermal stress. The component that expands more than the amount indicated by its CTE experiences thermal stress that is tensile, whereas the component that expands less than the amount indicated by its CTE experiences thermal stress that is compressive. The thermal stress is equal to the thermal force divided by the cross-sectional area. In the absence of an applied force,

$$F_1 + F_2 = 0 , \quad (8.9)$$

where  $F_1$  and  $F_2$  are the thermal forces in component 1 (all of the strips of component 1 together) and component 2 (all of the strips of component 2 together), respectively. Hence,

$$F_1 = -F_2 . \quad (8.10)$$

Since force is the product of stress and cross-sectional area, Eq. 8.10 can be written as

$$U_1 v_1 A = U_2 v_2 A , \quad (8.11)$$

where  $U_1$  and  $U_2$  are the stresses in components 1 and 2, respectively, and  $A$  is the area of the overall composite. Dividing by  $A$  gives

$$U_1 v_1 = U_2 v_2 . \quad (8.12)$$

Using Eq. 8.2, the strain in component 1 is given by  $(\alpha_c - \alpha_1)\Delta T$  and the strain in component 2 is given by  $(\alpha_c - \alpha_2)\Delta T$ . Since stress is the product of the strain and the modulus, Eq. 7.12 becomes

$$(\alpha_c - \alpha_1)\Delta T M_1 v_1 = -(\alpha_c - \alpha_2)\Delta T M_2 v_2 , \quad (8.13)$$

where  $M_1$  and  $M_2$  are the elastic moduli of components 1 and 2, respectively. Dividing Eq. 8.13 by  $\Delta T$  gives

$$(\alpha_c - \alpha_1)M_1 v_1 = -(\alpha_c - \alpha_2)M_2 v_2 . \quad (8.14)$$

Rearrangement gives

$$\alpha_c = (\alpha_1 M_1 v_1 + \alpha_2 M_2 v_2) / (M_1 v_1 + M_2 v_2) . \quad (8.15)$$

Equation 8.15 is the rule of mixtures expression for the CTE of a composite in the parallel configuration.

In the case that  $M_1 = M_2$ , Eq. 8.15 becomes

$$\alpha_c = (\alpha_1 v_1 + \alpha_2 v_2) / (v_1 + v_2) = \alpha_1 v_1 + \alpha_2 v_2 , \quad (8.16)$$

since

$$v_1 + v_2 = 1 . \quad (8.17)$$

If there are three components instead of two components in the composite, Eq. 8.9 becomes

$$F_1 + F_2 + F_3 = 0 , \quad (8.18)$$

and Eq. 8.17 becomes

$$v_1 + v_2 + v_3 = 1 , \quad (8.19)$$

but the method of deriving the rule of mixtures expression is the same.

## 8.2 Specific Heat

The heat capacity of a material is defined as the heat energy required to increase the temperature of the entire material by 1°C. The units of specific heat are commonly  $\text{J K}^{-1}$ . The specific heat (also known as the specific heat capacity) is defined as the heat energy required to increase the temperature of a unit mass of the material by 1°C. The units of specific heat are commonly  $\text{J g}^{-1} \text{K}^{-1}$ . Hence, the specific heat is the heat capacity divided by the mass of the material. However, this distinction between heat capacity and specific heat is not strictly followed by many authors.

The specific heat of a composite can be calculated from those of the components of the composite. Consider that the composite has a component 1 of specific heat  $c_1$  and mass fraction  $f_1$ , and a component 2 of specific heat  $c_2$  and mass fraction  $f_2$ . Let  $M$  be the total mass of the composite. Hence, the mass of component 1 is  $f_1M$ , and the mass of component 2 is  $f_2M$ . The heat absorbed per K rise in temperature is  $c_1f_1M$  for component 1, and is  $c_2f_2M$  for component 2.

The specific heat  $c_c$  of the composite is the total heat absorbed per °C rise in temperature divided by the total mass. Hence,

$$c_c = (c_1f_1M + c_2f_2M)/M = c_1f_1 + c_2f_2 . \quad (8.20)$$

Equation 8.20 implies that the specific heat of the composite is the weighted average of the specific heats of the components, where the weighting factors are the mass fractions of the components. This equation is a manifestation of the rule of mixtures. Note that the derivation of this equation does not require any particular distribution of the two components.

Kinetic energy is stored in a material through the vibrations of the crystal lattice and molecules and the rotations of molecules. Each way of vibrating or rotating is said to be a degree of freedom. Heat is needed to increase the temperature of a material because the kinetic energy per degree of freedom needs to increase as the temperature increases. The more degrees of freedom, the greater the specific heat of the material. Figure 8.3 shows the various vibrational modes in graphite.

For solids, the specific heat refers to that at a constant pressure (abbreviated  $c_p$ ), unless noted otherwise. This is because the pressure is usually fixed when using solid materials.

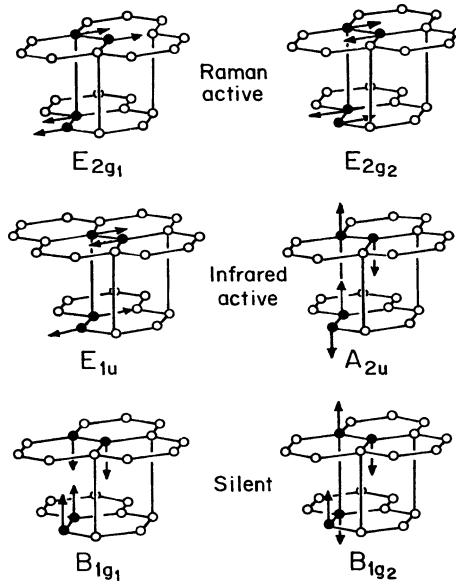


**Figure 8.3.** Various modes of vibration in graphite

**Table 8.2.** Specific heat values ( $c_p$ ) of various materials

Material	$c_p$ ( $\text{J g}^{-1} \text{K}^{-1}$ )
Water (25°C)	4.1813
Ice (-10°C)	2.050
Paraffin wax	2.5
Magnesium	1.02
Aluminum	0.897
Graphite	0.710
Diamond	0.5091
Glass	0.84
Silica (fused)	0.703

Table 8.2 shows a comparison of the  $c_p$  values for various materials.  $c_p$  is higher for water than ice. This is because there are more degrees of freedom for vibrations/rotations in the liquid, which has a disordered structure, than in the ordered structure of ice.  $c_p$  of paraffin wax is higher than that of ice, due to the disordered structure of solid wax, which is a molecular solid. Magnesium has a higher  $c_p$  than aluminum (which is next to magnesium in the periodic table of the elements), because it has a hexagonal crystal structure. In contrast, aluminum has a cubic (fcc) crystal structure. A hexagonal structure is less symmetrical than a cubic structure, resulting in more modes of lattice vibration. Similarly, graphite (hexagonal) has a higher  $c_p$  than diamond (cubic), even though graphite and diamond are both 100% carbon. Glass has a higher  $c_p$  than fused silica due to the lower degree of

three-dimensional networking in glass, meaning that there are more degrees of freedom for vibrations.

A material with a high specific heat may be used for thermal energy storage. An increase in temperature causes the storage of energy (which is the energy needed to raise the temperature of the material), while a decrease in temperature causes the release of this stored energy. A building should be designed to have a high heat capacity (known as the thermal mass in this context, so as to be distinguished from the specific heat) so that the temperature of the building does not change readily as the outdoor temperature changes. Thus, building materials of high specific heat are valuable. They include gypsum ( $1.09, \text{J g}^{-1} \text{K}^{-1}$ ), asphalt ( $0.92, \text{J g}^{-1} \text{K}^{-1}$ ), concrete ( $0.88, \text{J g}^{-1} \text{K}^{-1}$ ) and brick ( $0.84, \text{J g}^{-1} \text{K}^{-1}$ ).

## 8.3 Phase Transformations

### 8.3.1 Scientific Basis

A phase is a physically homogeneous region of matter. Different phases differ in structure. For example, ice and liquid water are different phases due to their different structures. A phase transformation, also known as a phase transition, refers to the change in phase upon changing the temperature/pressure. For example, the melting of ice to form liquid water is a phase transition. A phase transition is usually reversible. Indeed, liquid water freezes upon cooling.

The melting temperature limits the applicable temperature range of a solid material. However, below the melting temperature, there can be other limits. In the case of a solid that is at least partially amorphous (i.e., not completely crystalline) and an application in which high stiffness is required, the glass transition temperature ( $T_g$ ) is a temperature limit. Upon heating, a solid that is at least partially amorphous softens (i.e., the modulus reduces) at  $T_g$ , because the amorphous part in it softens. The softening at  $T_g$  is due to the movements of the constituent molecules, ions or atoms above  $T_g$ . Below  $T_g$ , there is not enough thermal energy for such movements to occur. This phase transition is reversible. Upon cooling, the modulus increases at  $T_g$  because the molecules, ions or atoms cannot move below  $T_g$ .  $T_g$  is below the melting temperature.

Amorphous materials (also known as glassy materials and noncrystalline materials) are commonly polymers and ceramics. Metals can be amorphous, but they are usually 100% crystalline. To make an amorphous metal it is necessary to cool the liquid metal at an extremely fast cooling rate so that there is insufficient time for the atoms to order and form a crystalline phase. On the other hand, polymers and ceramics involve ionic/covalent units that are much larger than atoms, and the ordering of these units to form a crystalline phase is relatively difficult. As a result, polymers and ceramics are commonly partially amorphous, if not completely amorphous.

**Table 8.3.** Glass transition temperatures  $T_g$  of various materials

Material	$T_g$ (°C)
Polyethylene (low-density) <sup>a</sup>	-105
Polypropylene (atactic) <sup>a</sup>	-20
Polypropylene (isotactic) <sup>a</sup>	0
Polyvinyl chloride <sup>a</sup>	81
Polystyrene <sup>a</sup>	95
Chalcogenide AsGeSeTe <sup>b</sup>	245
Soda lime glass <sup>b</sup>	520–600
Fused quartz <sup>b</sup>	1,175

<sup>a</sup>Polymer; <sup>b</sup> ceramic

Although the glass transition and melting are distinct phase transitions, both involve the movements of atoms, ions or molecules in the solid. These movements are more extensive during melting than during the glass transition. Therefore, a material that has a high melting temperature tends to have a high  $T_g$ .

Table 8.3 lists the  $T_g$  values of various polymers and ceramics. The  $T_g$  values are higher for ceramics than for polymers. This is consistent with the higher melting temperatures of ceramics.

Among the polymers, polyethylene has a very low  $T_g$  because of an absence of functional groups that cause intermolecular interactions, and an absence of bulky side groups. The bulky side groups as well as the intermolecular interactions hinder the sliding of molecules relative to one another. Polyvinyl chloride has a higher  $T_g$  because of the chloride functional group in its structure, which promotes intermolecular interactions. Polystyrene has an even higher  $T_g$  because of its bulky benzene side group. Isotactic polypropylene (with the  $-\text{CH}_3$  side groups of different mers on the same side of the polymer molecular chain) has a higher  $T_g$  than atactic polypropylene (with the  $-\text{CH}_3$  side groups of different mers positioned randomly on both sides of the polymer molecular chain) because the former is associated with more order and hence better packing of the molecular chains relative to one another. The better packing hinders the sliding of molecules relative to one another, thus causing a higher  $T_g$ .

Isotactic polypropylene is a commonly used thermoplastic polymer. The addition of rubber to it results in a composite that is tough and flexible. Polypropylene–polyethylene copolymers (with two types of mer in the same molecule) are attractive because the presence of the polyethylene component increases the low temperature impact. A shortcoming of polypropylene is its tendency to degrade upon exposure to ultraviolet (UV) radiation. In order to increase the UV resistance, carbon black can be added as a filler that absorbs the UV radiation.

Among ceramics, fused quartz has a higher  $T_g$  than soda lime glass. This is consistent with the higher melting temperature of fused quartz.

A chalcogenide is a compound with at least one chalcogen ion (sulfur, selenium or tellurium: all elements in Group IV of the periodic table) and at least one element that is more electropositive. For example, AsGeSeTe is a chalcogenide that has Se

and Te as chalcogens and As and Ge as electropositive elements. Another example is AgInSbTe, where Te is the chalcogen and Ag, In and Sb are the electropositive elements.

The  $T_g$  values of chalcogenides make these materials suitable for use in phase-change memory (abbreviated PCM, PRAM, PGRAM, chalcogenide RAM or C-RAM), which is a non-volatile computer memory that functions by switching between crystalline and amorphous states upon heating. Heating can change an amorphous material to a crystalline material because the amorphous state is a metastable state (a state that is not the lowest energy state, though it is not unstable), whereas the crystalline state is the thermodynamically stable state (the state with the lowest energy). On the other hand, the change of a crystalline state to an amorphous state requires melting and then rapid cooling. The cooling must be quick enough to avoid the formation of the crystalline state from the melt.

AgInSbTe is commonly used for rewritable optical discs (CDs). The writing process involves switching from the crystalline state to the amorphous state, which has low reflectivity, thereby storing the information optically. This involves (i) initially erasing the disc by switching the surface to the crystalline state through long, low-intensity laser irradiation (avoiding melting), (ii) heating the spot with short (less than 10 ns) high-intensity laser pulses to achieve local melting, and (iii) rapidly cooling the molten spot to transform it to the amorphous state.

A phase transition is known as a first-order phase transition if it involves the absorption or release of latent heat during the transition. The units of latent heat are joules (J). Latent heat is also known as the heat of transformation. The specific latent heat (often loosely called the latent heat) is the latent heat per unit mass, so its units are J/g. During the transformation, the temperature stays constant as the latent heat is absorbed or released. For example, latent heat of fusion is absorbed during melting and latent heat of solidification is released during freezing. A process that absorbs latent heat is said to be endothermic, while a process that evolves latent heat is said to be exothermic. All spontaneous reactions are exothermic.

The latent heat is due to the difference in heat content (also known as the enthalpy) between the initial and final states of the phase transition. The heat content is higher for the liquid state than for the solid state because the atoms, ions or molecules are slightly more separated in the liquid state than in the solid state, and energy is needed to cause this separation. The greater the energy required to cause the separation, the higher the latent heat of fusion. For the same material, the latent heat of vaporization is much higher than that of fusion. For example, the specific latent heat of fusion of lead is 24.5 J/g, whereas the specific latent heat of vaporization of lead is 871 J/g. This difference is due to the much greater change in the degree of separation required for a liquid to boil (i.e., to change from liquid to vapor, where the vapor has a much lower density than the liquid) than that required for a solid to melt (i.e., to change from solid to liquid; in other words, the density difference between the solid and the liquid is small compared to the density difference between the liquid and the vapor). Latent heat is absorbed when a solid melts and latent heat is released when a solid freezes. The specific latent heat of fusion of carbon dioxide is high (184 J/g), whereas it is low for nitrogen

(25.7J/g). This is because of the stronger intermolecular attractions in carbon dioxide compared to nitrogen.

A phase transition that does not involve a latent heat is known as a second-order phase transition or a continuous phase transition. The glass transition is an example of such a transition. The glass transition involves no latent heat because there is no difference in heat content between the initial state (the amorphous solid state) and the final state (the softened state). The transition between ferromagnetic and paramagnetic states is another example of a second-order phase transition.

The latent heat associated with a first-order phase transition provides a mechanism for the storage of thermal energy. For example, energy is stored during melting (when the ambient temperature is above the melting temperature) and released during freezing (when the ambient temperature is below the freezing temperature). A material with a melting temperature that is near room temperature and placed outdoors can be used to store energy during the day (when the outside temperature is above room temperature) and release energy during the night (when the outside temperature is below room temperature). Such a material is known as a phase-change material (abbreviated to PCM; note that this should not be confused with phase-change memory, which has the same abbreviation). Wax is an example of a phase-change material.

Due to the difference in kinetics between the melting and freezing transitions, the melting temperature and the freezing temperature may not be equal. Freezing changes a liquid to a crystalline solid, the formation of which requires the ordering of atoms, ions or molecules. The ordering process can be hastened if freezing is allowed to occur on a crystalline solid surface, which serves as a seed for crystallization. Hence, the freezing of a liquid is facilitated by the presence of seed crystals (called nuclei) around which the liquid freezes. Thus, in the absence of nuclei, a liquid can remain a liquid (called a supercooled liquid) below the equilibrium freezing temperature (the freezing temperature in the case of infinitely slow cooling, which provides plenty of time for freezing to take place, and where kinetics do not affect the outcome). For example, droplets of supercooled water in the clouds may change to ice upon being hit by the wings of a passing airplane. The ice formed on the wings can cause problems with lift. Freezing rain is also supercooled water droplets, which become ice upon hitting a solid surface.

The supercooling  $\Delta T$  is defined as

$$\Delta T = \text{melting temperature} - \text{freezing temperature} . \quad (8.21)$$

When the supercooling is positive, the freezing temperature is below the melting temperature. This is usually due to the sluggishness of the freezing. When the supercooling is negative, the freezing temperature is above the melting temperature. Negative supercooling occurs, but it is not well understood.

### 8.3.2 Shape Memory Effect

The shape memory effect (Sect. 3.6.3) involves a phase transformation (called a martensitic transformation) that changes the material from the austenite phase

(cubic) to the martensite phase (typically tetragonal). Due to the change in crystal structure, the martensitic transformation is accompanied by twinning, meaning that the martensite that forms from the austenite is heavily twinned, as illustrated in Figs. 8.4 and 8.5.

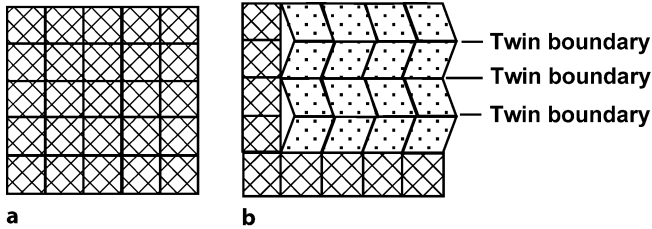


**Figure 8.4.** **a** Austenite, **b** austenite (cross-hatched region) coexisting with martensite (dotted region), which is twinned. The change in lattice parameters upon changing from austenite to martensite is exaggerated in **(b)** for the sake of clarity

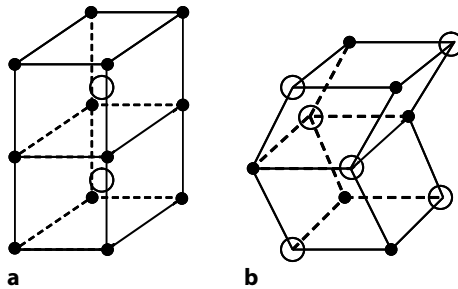


**Figure 8.5.** Typical crystal structures of a shape memory alloy in the form of an AB compound, with A atoms shown by solid circles and B atoms shown by open circles. **a** Austenite, **b** twinned martensite, with the twin boundary being the horizontal plane

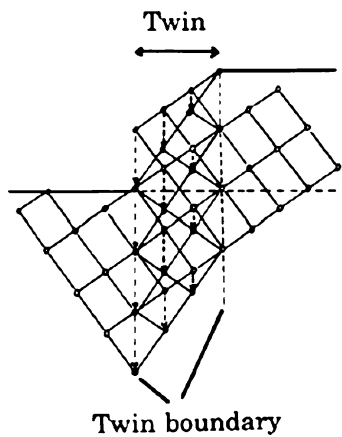


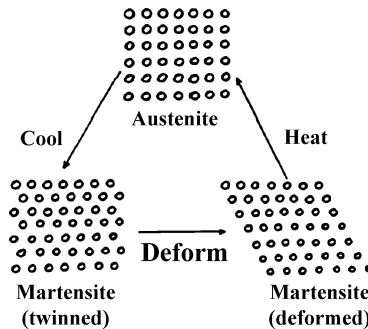
**Figure 8.6.** The formation of a twin

Twinning refers to the existence of a mirror plane in a material such that the parts of the material adjacent to the mirror plane are mirror images in terms of the positions of the atoms in them, as illustrated in Fig. 8.6, which shows two mirror planes (each of which is called a twin boundary). The region between the two twin boundaries is called the twin, and it differs in structure from the regions outside the twin. The arrows in Fig. 8.6 show the movements of the atoms during the twin formation. The atom movement means deformation (i.e., strain).

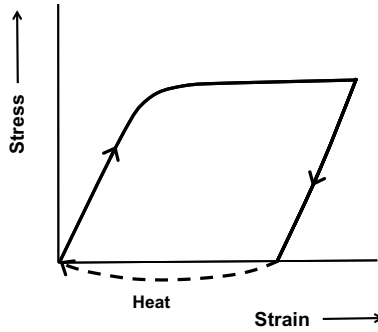
The martensite phase is special in that it is highly twinned, thus allowing it to undergo reversible strain that is beyond the elastic limit. This phenomenon is known as pseudoplasticity or superplasticity. If the strain is restrained, stress is provided. Thus, the shape memory effect can be used to provide strain and/or stress; i.e., it serves as an actuator. Upon the subsequent return from the martensite phase to the austenite phase (i.e., the reverse of the martensitic transformation), the original shape (i.e., nearly zero strain) returns.

Figure 3.33a shows pseudoplastic behavior. It involves the use of stress to induce the change from the austenite phase to the martensite phase. Applications include orthodontal braces, bone plates, eyeglass frames, medical tools, cellular phone antennae, and bra underwiring. In case of an orthodontal brace, the brace is installed in a patient in the state corresponding to the upper (loading) plateau in Fig. 3.33a. The lower (unloading) plateau then allows the stress to be maintained at a roughly constant value as the strain is gradually decreased (i.e., as the teeth are gradually pulled together by the brace). It is important for the stress to be maintained during the course of this dental treatment. Similarly, for a bone plate that is used to fasten pieces of broken bones, it is important for the stress to be maintained as the fracture gradually heals.

The martensitic transformation can be induced by cooling instead of the application of stress. After cooling, the martensite phase is deformed to a new shape. Subsequent heating returns the martensite phase to the austenite phase. This change in phase means a return to the shape associated with the original austenite.



**Figure 8.7.** The shape memory effect that involves cooling from austenite to form martensite, deformation of the martensite, and then heating to change the martensite back to austenite. The return to the austenite phase brings a return to the shape of the austenite (i.e., the shape prior to the deformation)



**Figure 8.8.** The stress–strain curve during the deformation of a shape memory alloy in the form of martensite (below  $A_s$ ). Heating subsequent to the deformation returns the strain to zero (i.e., the original shape)

The shape memory effect is illustrated in Fig. 8.7, which shows that austenite (the initial phase) transforms to a martensite upon cooling, which is heavily twinned. The martensite is then mechanically deformed to a particular shape. After this, the deformed martensite is heated so that it transforms back to austenite. The reverse transformation is accompanied by a return to the original shape of the austenite (i.e., the shape prior to the deformation). This effect is further illustrated in Fig. 8.8, where the starting point is martensite. The loading part of the stress–strain curve shows the deformation of the martensite. After subsequent unloading, heat is applied to change the martensite back to austenite. This change of phase results in the restoration of the shape of the austenite; i.e., the state prior to deformation (or strain = 0).

As shown in Fig. 8.9, the temperature at which the transformation from austenite to martensite begins upon cooling is denoted  $M_s$ . The temperature at which the martensitic transformation is completed upon cooling is denoted  $M_f$ . Obviously,  $M_f$  is below  $M_s$ . The temperature at which the transformation from martensite to austenite begins upon heating is denoted  $A_s$ . The temperature at which the transformation from martensite to austenite finishes upon heating is denoted  $A_f$ . Again, obviously  $A_f$  is above  $A_s$ . Due to hysteresis,  $M_s$  tends to be less than  $A_s$ , though it is usually close to  $A_s$ .

Figure 8.8 is the behavior below  $A_s$ , since it describes the deformation of the martensite. If the stress after unloading is continued into the negative regime without heating, ferroelasticity (Fig. 3.33b) results, provided that there are two states of twinning that allow the positive stress plateau and the negative stress plateau.

The values of these four temperatures defined in Fig. 8.9 depend on the stress, as illustrated in Fig. 8.10. Due to the dependence on the stress, at a fixed temperature austenite changes to martensite upon increasing the stress. The pseudoplastic behavior shown in Fig. 3.33a is based on this stress-induced martensitic transformation; it occurs at temperatures above  $A_f$ , so that applying stress causes the change from austenite to martensite.

The values of these four temperatures defined in Fig. 8.9 may shift upon repeated use of the shape memory effect. This shift is known as functional fatigue and is due to microstructural changes upon multiple cycles of the effect.

The various manifestations of the shape memory effect are illustrated in Fig. 8.11. These manifestations depend on the temperature. The effect in Fig. 8.11a is the same as that in Fig. 8.8 and occurs at temperatures below  $A_s$ , with the deformation shown in the stress–strain curve being that of martensite. The effect shown in Fig. 8.11b occurs at temperatures above  $A_f$  (i.e., when the phase is austenite prior to deformation) and relates to pseudoelasticity; it is the same as the effect shown in Fig. 3.33a, except that, for the sake of simplicity, it does not show any degree of strain irreversibility after unloading. The effect in Fig. 8.11c occurs at temperatures between  $A_s$  and  $A_f$  and shows characteristics that are intermediate between those shown in Fig. 8.11a and b. In this intermediate temperature range, austenite and martensite coexist, with the martensite portion undergoing the effect shown in Fig. 8.11a and the austenite portion undergoing the effect depicted in Fig. 8.11b.

The shape memory effect shown in Fig. 8.8 (i.e., Fig. 8.11a) is valuable for numerous applications. Examples of its application are self-expandable cardiovascular stents, blood clot filters, engines, actuators, flaps that change the direction of air flow depending on the temperature (for air conditioners and aircraft), and couplings. Some of these applications are described below. However, applications to robotics have problems due to energy inefficiency, slow response, and large hysteresis.

A stent is used to reinforce weak vein walls and to widen narrow veins. It can be introduced in a chilled deformed shape; i.e., a scaffold with a relatively small diameter. During deployment, the stent travels through the arteries. After deployment, due to the warmth from the body, the stent expands to the appropriate diameter with sufficient force to open the vessel lumen and reinstate blood flow. Such a stent replaces similar stainless steel stents that are expanded with a little balloon.

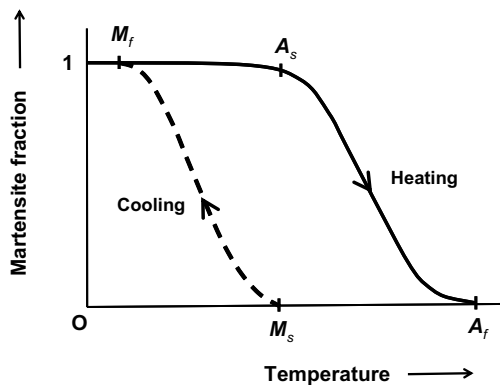


**Figure 8.9.** Decrease in the martensite fraction during heating, and the increase in this fraction during subsequent cooling

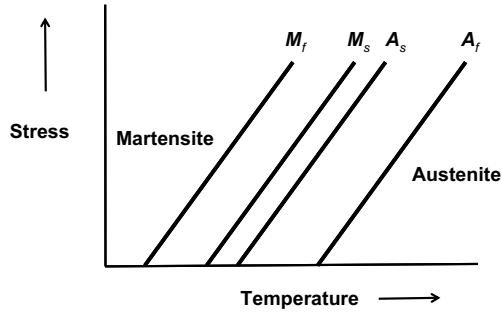


**Figure 8.10.** Effect of stress on the start and finish temperatures of the change from austenite to martensite ( $M_s$  and  $M_f$ ) and the start and finish temperatures of the change from martensite to austenite ( $A_s$  and  $A_f$ )

A shape memory coupling for connecting two tubes is placed over the joint area in an expanded state, so that it fits over the tubing (Fig. 8.12a and b). Upon subsequent heating, it shrinks back to its original diameter, thereby squeezing the tubing and providing a tight fit (Fig. 8.12c).

Examples of shape memory alloys (abbreviated to SMAs) are copper-zinc-aluminum, copper-aluminum-nickel and nickel-titanium alloys. NiTi with 50 at.% Ti is known as nitinol, which stands for nickel titanium Naval Ordnance Laboratory (the place where it was discovered). NiTi alloys are generally more expensive and exhibit better mechanical properties than copper-based SMAs. Disadvantages

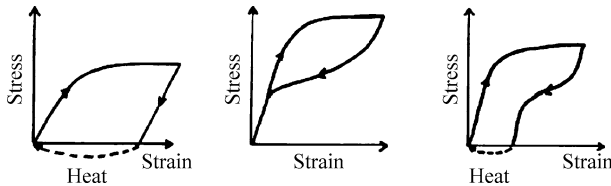


**Figure 8.11.** Manifestations of the shape memory effect, depending on the temperature. **a** Temperatures below  $A_s$ , as shown in Fig. 8.7, **b** temperatures above  $A_f$ , as shown in Fig. 3.33a, **c** temperatures between  $A_s$  and  $A_f$ , showing behavior intermediate between those shown in (a) and (b)

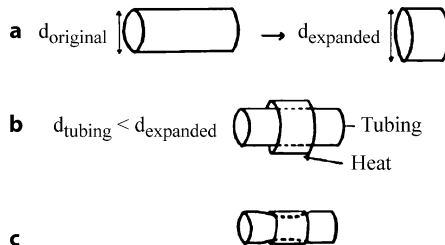


**Figure 8.12.** The use of the shape memory effect (Fig. 8.7) to achieve a coupling that fits tightly around tubing. **a** Deformation of the martensite to cause expansion of the coupling, **b** fitting the expanded coupling around the tubing, **c** heating to change the martensite back to austenite, thereby restoring the coupling its original, undeformed shape with a smaller diameter

of shape memory alloys include high cost, poor machinability and poor fatigue resistance compared to steel.

### 8.3.3 Calorimetry

Investigations of phase transitions are commonly conducted by calorimetry, which allows the transition temperature to be measured during heating and cooling, and the latent heat of the transformation during heating and cooling. A first-order transition gives a peak in the heat flow vs. temperature plot such that the area under the peak is the latent heat of the transformation. In contrast, a second-order transition does not give a peak, just a change in slope in this plot, due to the absence of latent heat.

One widely used form of calorimetry is differential scanning calorimetry (DSC), which involves scanning the temperature at a controlled heating/cooling rate, while the temperature of the specimen is kept the same as a reference (typically an empty pan). At a first-order phase transition, the absorption or release of latent heat from the specimen means that the calorimeter must add heat to or remove heat from the specimen in order to maintain the specimen and the reference at the same temperature as the temperature is scanned. The amount of heat applied or removed is the latent heat, which is therefore measured.

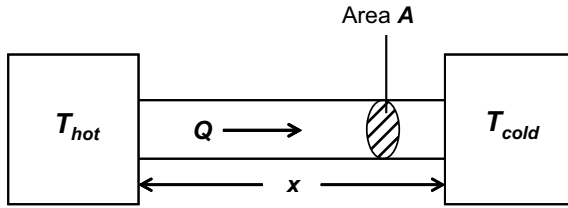
An alternative form of DSC involves measuring the temperature difference between the specimen and the reference when the two are subjected to the same constant heating/cooling rate. The higher the heat capacity of the specimen compared to that of the reference, the greater the amount of heat that needs to be applied to the specimen in order to maintain the specimen and reference at the same constant heating/cooling rate. The application of heat gives rise to a small temperature difference between the specimen and the reference.

## 8.4 Thermal Conductivity

The thermal conductivity ( $k$ ) is a material property that describes the ability of the material to conduct heat. It is defined as

$$\Delta Q/\Delta t = kA(\Delta T/x), \quad (8.22)$$

where  $Q$  is the heat (with units of J),  $t$  is the time,  $\Delta Q/\Delta t$  is the heat flow (i.e., the amount of heat flowing per unit time),  $A$  is the cross-sectional area of the material perpendicular to the direction of heat flow, and  $\Delta T$  is the temperature difference between the two ends of the material of length  $x$  in the direction of heat flow, as illustrated in Fig. 8.13, where one-dimensional heat flow is assumed (i.e., there is no loss of heat to the surrounding). The temperature gradient is  $\Delta T/x$ . Equation 8.22 means that the thermal conductivity is the heat flow per unit cross-sectional area per unit temperature gradient; i.e., the heat flux per unit temperature gradient. The heat flow per unit cross-sectional area is also called the heat flux. Since  $W = J/s$ , the units of  $k$  are  $W/(mK)$ , which are the same as  $W/(m^{\circ}C)$ .



$$\Delta T = T_{hot} - T_{cold}$$

**Figure 8.13.** Heat flowing from the hot end to the cold end of a material of cross-sectional area  $A$  and length  $x$

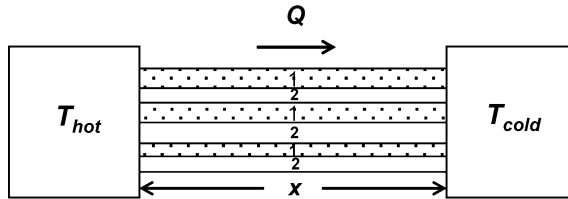


**Figure 8.14.** A thermal conductor in the form of a composite with components labeled 1 (dotted regions) and 2 (white regions) in the form of strips that are parallel and oriented in the direction of heat flow

The thermal conductivity of a composite ( $k_c$ ) can be calculated from the thermal conductivities and volume fractions of each of the components (labeled 1 and 2) in the composite. Consider the case where the components are positioned in parallel, as shown in Fig. 8.14. The heat flow in component 1 (all the strips of component 1 together) plus that in component 2 (all the strips of component 2 together) equals the heat flow in the overall composite. Hence, based on Eq. 8.22,

$$k_1 A_1 (\Delta T/x) + k_2 A_2 (\Delta T/x) = k_c A (\Delta T/x) , \tag{8.23}$$

where  $k_1$  and  $k_2$  are the thermal conductivities of components 1 and 2 respectively,  $A_1$  and  $A_2$  are the cross-sectional areas (all the strips of each component considered together) of components 1 and 2, respectively, and  $A$  is the cross-sectional area of the overall composite. Obviously,

$$A = A_1 + A_2 . \tag{8.24}$$

Eq. 8.23 can be rewritten as

$$k_c = (k_1 A_1/A) + (k_2 A_2/A) = v_1 k_1 + v_2 k_2 , \tag{8.25}$$

where  $v_1 = A_1/A$  and is the volume fraction of component 1, and  $v_2 = A_2/A$  and is the volume fraction of component 2. Equation 8.25 is the rule of mixtures for the parallel configuration.

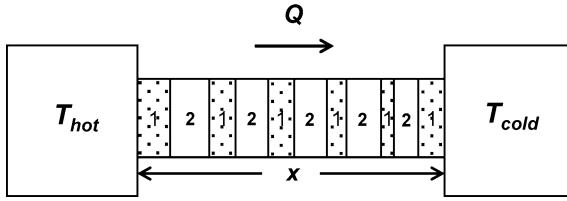


**Figure 8.15.** A thermal conductor in the form of a composite with components labeled 1 (*dotted regions*) and 2 (*white regions*) in the series configuration; i.e., the components are in the form of strips that are parallel and oriented perpendicular to the direction of heat flow

Next, consider the case where the components are in series, as shown in Fig. 8.15. The temperature difference between the two ends of the composite is given by

$$\Delta T = \Delta T_1 + \Delta T_2, \quad (8.26)$$

where  $\Delta T_1$  is the contribution to the temperature difference from component 1 (all the strips of component 1 together) and  $\Delta T_2$  is the contribution to the temperature difference from component 2 (all the strips of component 2 together). Based on Eq. 8.22, Eq. 8.26 becomes

$$(\Delta Q/\Delta t) [x_1/(k_1 A)] + (\Delta Q/\Delta t) [x_2/(k_2 A)] = (\Delta Q/\Delta t) [x/(k_c A)], \quad (8.27)$$

assuming that both components have the same cross-sectional area  $A$ . Simplification of Eq. 8.27 gives

$$x_1/k_1 + x_2/k_2 = x/k_c. \quad (8.28)$$

Dividing by  $x$  gives

$$v_1/k_1 + v_2/k_2 = 1/k_c, \quad (8.29)$$

where  $v_1 = x_1/x$  is the volume fraction of component 1, and  $v_2 = x_2/x$  is the volume fraction of component 2. Equation 8.29 is the rule of mixtures for the series configuration.

The thermal resistivity is defined as the reciprocal of the thermal conductivity. Thus, the units of thermal resistivity are mK/W. From Eq. 8.22, the thermal resistivity  $1/k$  is given by

$$1/k = [A(\Delta T/x)]/(\Delta Q/\Delta t). \quad (8.30)$$

In other words, the thermal resistivity is the temperature gradient divided by the heat flux.

The thermal resistance is defined as the temperature gradient divided by the heat flow (not flux). Hence, it is given by the thermal resistivity divided by the cross-sectional area  $A$ :

$$\text{Thermal resistance} = 1/(kA) = (\Delta T/x)/(\Delta Q/\Delta t). \quad (8.31)$$

The units of thermal resistance are  $K/(m W)$ . In the series configuration (Fig. 8.14), the thermal resistance of the composite is the weighted sum of the thermal resistances of the two components:

$$v_1/(k_1A) + v_2/(k_2A) = 1/(k_cA) , \quad (8.32)$$

which, upon canceling  $A$ , is the same as Eq. 8.29.

The conduction of heat can involve the movement of electrons and/or phonons (vibrational waves) from the hot point to the cold point, since electrons and phonons are both associated with kinetic energy. Due to the abundance of mobile electrons in them, metals are good thermal conductors. Diamond and cubic boron nitride are even more thermally conductive than metals in spite of their absence of mobile electrons, as evidenced by the fact that they are electrical insulators. The high thermal conductivities of diamond and cubic boron nitride are due to the high mobility of the phonons in them, which is in turn due to the low masses of the atoms in these materials (carbon in the case of diamond).

The thermal conductivity values of various materials, including both thermal conductors and thermal insulators, are listed in Table 8.4. The best thermal conductors are diamond and cubic boron nitride, but these materials are very expensive. Other than these exceptional materials, the best thermal conductors are metals, particularly silver and copper. Brass (Cu-Zn alloy) has a much lower thermal conductivity than copper due to the zinc alloying element, which causes electron scattering. Similarly, the thermal conductivity is lower for carbon steel than iron due to the carbon alloying element in the steel. Beryllium oxide and aluminum nitride are comparable in terms of thermal conductivity to metals, though their values are much lower than those of cubic boron nitride and diamond. Hexagonal boron nitride is less thermally conductive than aluminum nitride or beryllium oxide. Other than cubic/hexagonal boron nitride, beryllium oxide and aluminum nitride, ceramics are typically thermal insulators rather than thermal conductors because of the inadequate numbers of mobile electrons and phonons in them, as shown by the low thermal conductivities of fused silica, mica, fiberglass, vermiculite (a clay mineral), and perlite (a volcanic glass, mainly comprising  $SiO_2$ ).

The thermal conductivity of a material varies with the temperature. The values in Table 8.4 are at or near room temperature. For a metal, the free (mobile) electrons govern both the thermal conductivity ( $k$ ) and the electrical conductivity ( $\sigma$ ), which are thus proportional to one another. The relationship, known as the Wiedemann–Franz Law, is

$$k/\sigma = LT , \quad (8.33)$$

where  $T$  is the temperature in K (Kelvin) and  $L$  is a constant equal to  $2.44 \times 10^{-8} W \cdot \Omega/K^2$ . Equation 8.33 means that, as the temperature increases,  $k$  increases and  $\sigma$  decreases. The increase in  $k$  with increasing temperature occurs because the average particle (electron) velocity increases with temperature, and this increase in velocity enhances the forward transport of energy. The decrease in  $\sigma$  with increasing temperature arises because an increase in temperature causes more scattering of the electrons. At low temperatures, a metal tends to be a poor thermal conductor but a good electrical conductor.

For copper at room temperature ( $25^{\circ}\text{C} = 298\text{ K}$ ),  $\sigma = 0.596 \times 10^8 \Omega^{-1} \text{ m}^{-1}$  (Table 6.2) and  $k = 401 \text{ W}/(\text{m K})$  (Table 8.4). Substitution of these values into Eq. 8.33 gives  $L = 2.26 \times 10^{-8} \text{ W}\Omega/\text{K}^2$ . The theoretical value of  $L$  is  $2.44 \times 10^{-8} \text{ W}\Omega/\text{K}^2$ .

Metals and graphite are thermally and electrically conductive. Thermal conductors that are electrically insulating are needed for heat dissipation from microelectronics. For example, the encapsulation of an integrated circuit component needs to be electrically insulating, but thermal conductivity will help to dissipate the heat from the electronic package. A combination of high thermal conductivity and high electrical resistivity is provided by diamond, cubic boron nitride, beryllium oxide and aluminum nitride, and to a lesser extent in terms of the thermal conductivity, hexagonal boron nitride.

**Table 8.4.** Thermal conductivities of various materials, including thermal conductors and thermal insulators

Material	Thermal conductivity (W/(mK))
Diamond	2,000
Boron nitride (cubic)	1,700
Silver	429
Copper	401
Beryllium oxide (BeO)	325
Aluminum	250
Aluminum nitride	140–180
Molybdenum	138
Brass	109
Nickel	91
Iron	80
Cast iron	55
Carbon steel	54
Boron nitride (hexagonal)	33
Monel (Cu-Ni alloy)	26
Alumina	18
Zirconia (yttria stabilized)	2
Carbon	1.7
Fused silica	1.38
Window glass	0.96
Mica	0.71
Nylon 6	0.25
Paraffin wax	0.25
Machine oil	0.15
Straw insulation	0.09
Vermiculite	0.058
Paper	0.05
Rock wool insulation	0.045
Fiberglass	0.04
Styrofoam	0.033
Perlite (1 atm)	0.031
Air	0.024
Perlite (vacuum)	0.00137

## 8.5 Thermal Conductance of an Interface

An interface is associated with a thermal resistance in the direction perpendicular to the interface. This thermal resistance relates to the temperature difference across the interface per unit heat flow. Its units are K/W. The greater the thermal resistance of the interface, the higher the temperature difference across the interface for the same heat flow. It should be distinguished from the thermal resistance of a volume (which has different units of K/(m W); see Sect. 8.4).

The thermal resistance of an interface is inversely proportional to the area of the interface. Thus, a more scientifically meaningful quantity that is independent of the area of the interface is the thermal resistivity of the interface, defined as

$$\begin{aligned} \text{Thermal resistivity of interface} &= (\text{thermal resistance of interface}) \\ &\times (\text{area of interface}) . \end{aligned} \quad (8.34)$$

In other words, the thermal resistivity of an interface is the temperature difference across the interface per unit heat flux. The units of thermal resistivity are  $\text{m}^2 \text{K/W}$ .

The thermal conductance of an interface is defined as the reciprocal of the thermal resistivity of the interface. Hence, the units of conductance are  $\text{W}/(\text{m}^2 \text{K})$ , which are different from the units of  $\text{W}/(\text{mK})$  for the thermal conductivity of a volume of material (Sect. 8.4).

Consider an interface that consists of two components, labeled 1 and 2, that have interfacial thermal resistivities of  $\rho_1$  and  $\rho_2$ , respectively, and interfacial areas of  $A_1$  (all the regions of component 1 together) and  $A_2$  (all the regions of component 2 together), respectively, as illustrated in Fig. 8.16. Since the thermal resistance  $R$  is the temperature difference  $\Delta T$  across the interface divided by the heat flow,

$$\text{Heat flow} = \Delta T/R . \quad (8.35)$$

The heat flow in component 1 plus that in component 2 equals that in the overall interface. Hence,

$$(\Delta T/R_c) = (\Delta T/R_1) + (\Delta T/R_2) , \quad (8.36)$$

where  $R_1$ ,  $R_2$  and  $R_c$  are the thermal resistances of component 1, component 2, and the overall interface respectively. Note that the temperature difference across the interface is the same for components 1 and 2. Simplifying Eq. 8.36 gives

$$1/R_c = (1/R_1) + (1/R_2) . \quad (8.37)$$

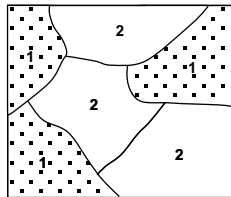


**Figure 8.16.** An interface in the form of a composite consisting of components labeled 1 (*dotted regions*) and 2 (*white regions*)

Since the thermal resistivity is the thermal resistance multiplied by the area, Eq. 8.37 can be written as

$$A_c/\rho_c = A_1/\rho_1 + A_2/\rho_2, \quad (8.38)$$

where  $A_1$ ,  $A_2$ , and  $A_c$  are the areas of component 1, component 2, and the overall interface, respectively. Dividing by  $A_c$  gives

$$1/\rho_c = a_1/\rho_1 + a_2/\rho_2, \quad (8.39)$$

where  $a_1$  and  $a_2$  are the area fractions of components 1 and 2, respectively. Equation 8.39 is the rule of mixtures expression for calculating the thermal resistivity of an interface that is a two-dimensional composite. The thermal conductance  $\sigma_c$  of the overall interface is given by

$$\sigma_c = 1/\rho_c. \quad (8.40)$$

Combining Eq. 8.39 and 8.40 gives

$$\sigma_c = a_1/\rho_1 + a_2/\rho_2 = a_1\sigma_1 + a_2\sigma_2, \quad (8.41)$$

where  $\sigma_1 (= 1/\rho_1)$  and  $\sigma_2 (= 1/\rho_2)$  are the thermal conductances of components 1 and 2, respectively. Equation 8.41 is the rule of mixtures expression for calculating the thermal conductance of an interface that is a two-dimensional composite.

## 8.6 Evaluating the Thermal Conduction

The most commonly used methods of evaluating the thermal conduction are the guarded hot plate method (a steady-state method) and the laser flash method (a transient method), as described below.

### 8.6.1 Guarded Hot Plate Method

Thermal conduction is most commonly evaluated using the guarded hot plate method (ASTM D5470), which involves measuring under a steady-state heat flux. The heat flux is provided by a heated block (e.g., a copper block with heating wires inside) and a cooled block (e.g., a copper block with running water inside). The heat flows from the heated block to the cooled block, as shown in Fig. 8.17. Between the heated block and the cooled block are two smaller conductor blocks made of a thermal conductor such as copper, and labeled conductor I and conductor II in Fig. 8.17. The specimen is sandwiched between conductors I and II. Each conductor has at least two drilled holes for inserting a thermocouple into each hole. In Fig. 8.17, the temperatures  $T_1$  and  $T_2$  are measured in conductor I and the temperatures  $T_3$  and  $T_4$  are measured in conductor II. Due to the thermal insulation surrounding the specimen and conductors I and II, the heat flow is assumed to be one-dimensional, with no loss of heat to the surroundings.

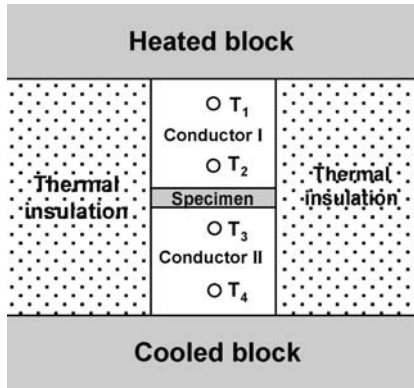


**Figure 8.17.** Guarded hot plate method of evaluating thermal conduction. The specimen is sandwiched between conductors I and II. Heat flows from the heated block to the cooled block

In an experiment, the equilibrium (state state) is assumed to have been obtained when  $T_1 - T_2$  and  $T_3 - T_4$  are essentially equal. The heat flow  $\Delta Q/\Delta t$  is given by

$$\Delta Q/\Delta t = kA\Delta T/d_A, \quad (8.42)$$

where  $d_A$  is the distance between thermocouples  $T_1$  and  $T_2$ ,  $A$  is the cross-sectional area of conductor I, and  $k$  is the thermal conductivity of conductor I.

The temperature at the bottom of conductor I (i.e., the temperature at the top surface of the specimen) is  $T_A$ , which is given by

$$T_A = T_2 - \frac{d_B}{d_A}(T_1 - T_2), \quad (8.43)$$

where  $d_B$  is the distance between thermocouple  $T_2$  and the top surface of the specimen. Similarly, the temperature at the bottom surface of the specimen is  $T_D$ , which is given by

$$T_D = T_3 + \frac{d_D}{d_C}(T_3 - T_4), \quad (8.44)$$

where  $d_D$  is the distance between thermocouple  $T_3$  and the bottom surface of the specimen, and  $d_C$  is the distance between thermocouples  $T_3$  and  $T_4$ .

The temperature difference between the top and bottom surfaces of the specimen is thus

$$\Delta T = T_A - T_D. \quad (8.45)$$

If the thermal resistance of the interface between the specimen and each of conductors I and II is ignored, the thermal resistance  $R$  of the specimen is given by

$$R = 1/(kA) = (\Delta T/x)/(\Delta Q/\Delta t), \quad (8.46)$$

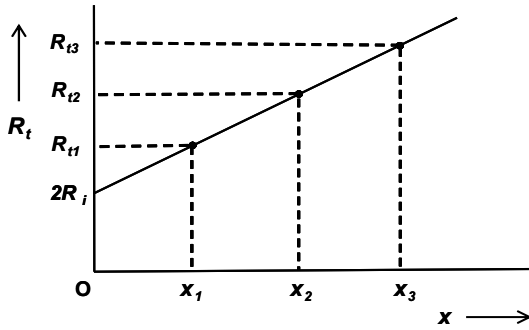


Figure 8.18. Variation of the total thermal resistance  $R_t$  with the thickness  $x$

where  $x$  is the specimen thickness,  $\Delta T$  is given by Eq. 8.45,  $\Delta Q/\Delta t$  is given by Eq. 8.42, and Eq. 8.31 has been used. The thermal conductivity  $k$  can be calculated from  $R$  and  $A$ .

However, the thermal resistance of the interface between the specimen and each of the conductors I and II cannot be ignored. Thus, the total thermal resistance  $R_t$  (i.e., the measured thermal resistance) is given by

$$R_t = R_s + 2R_i , \tag{8.47}$$

where  $R_s$  is the thermal resistance of the specimen and  $R_i$  is the thermal resistance of each interface. In order to determine  $R_s$ , specimens of at least three different known thicknesses should be measured. Figure 8.18 shows the plot of  $R_t$  vs.  $x$ . It is a straight line, with the  $R_t$  intercept being  $2R_i$  and the slope being the thermal resistance of the specimen material (of area  $A$ ) per unit thickness. The thermal resistance of the specimen material per unit thickness, multiplied by the specimen thickness under consideration, gives the thermal resistance of the specimen, which is equal to  $1/(kA)$ , where  $k$  is the thermal conductivity of the specimen. Thus,  $k$  can be determined from the slope of the plot of Fig. 8.18.

The plot in Fig. 8.18 also allows the determination of  $R_i$ , which depends on the roughness of the proximate surfaces of conductors I and II. The greater their roughness, the greater the volume of air voids at the interface, and the higher  $R_i$ . In addition,  $R_i$  depends on the ability of the specimen to conform to the surface topography of conductor I or II. The greater the conformability, the smaller the volume of air voids at the interface and the lower  $R_i$ .

Whether a thin interface material is placed at the interface between the proximate surfaces of conductors I and II or not, the two-dimensional thermal resistivity of the interface can be evaluated. If an interface material is present, the overall interface consists of (i) the interface material and (ii) the interfaces between the interface material and each of the two proximate surfaces. From Eq. 8.35, the two-dimensional thermal resistance  $R$  of this overall interface is given by

$$R = \Delta T/(\Delta Q/\Delta t) , \tag{8.48}$$

where  $\Delta T$  is experimentally obtained using the method of Fig. 8.17 and Eq. 8.45, and  $\Delta Q/\Delta t$  is experimentally obtained using the method of Fig. 8.17 and Eq. 8.42. From  $R$ , the two-dimensional thermal resistivity can be calculated using Eq. 8.34. The reciprocal of the thermal resistivity is the thermal conductance of the interface.

## 8.6.2 Laser Flash Method

The laser flash method is a transient (not steady-state) method of evaluating thermal conduction. It involves applying a flash of laser radiation to the surface of the specimen and then measuring the rate of temperature rise at the back surface of the specimen using a sensitive temperature measurement device (e.g., a thermocouple that is small enough to respond rapidly, or an infrared sensor) (Fig. 8.19). The laser flash provides a heat pulse. This heat is then conducted through the specimen from the front surface to the back surface. The higher the thermal diffusivity (defined below), the steeper the temperature rise at the back surface.

The thermal diffusivity ( $\alpha$ , not to be confused with CTE, which is also denoted by  $\alpha$ ) is defined as the ratio of the thermal conductivity ( $k$ ) to the volumetric specific heat ( $\rho c_p$ ). The volumetric specific heat is defined as the product of the specific heat ( $c_p$ , at constant pressure) and the density ( $\rho$ ). Since the specific heat is defined as the amount of heat required to increase the temperature by 1 K for a unit mass of a material, the multiplication of the specific heat by the density (which is the mass per unit volume) gives the amount of heat required to increase the temperature by 1°C for a unit volume of the material. Because the heat travels through a volume, it is more meaningful to consider the volumetric specific heat rather than the specific heat.

By definition, the thermal diffusivity is given by

$$\alpha = k/(\rho c_p) . \quad (8.49)$$

The units  $\alpha$  of are  $\text{m}^2/\text{s}$ , since the units of  $k$  are  $\text{W}/(\text{mK})$ ; the units of  $\rho$  are  $\text{g}/\text{m}^3$ ; and the units of  $c_p$  are  $\text{J}/(\text{gK})$ . The laser flash method gives  $\alpha$ , which allows  $k$  to be calculated using Eq. 8.49 provided that  $\rho$  and  $c_p$  are known.

Compared to the guarded hot plate method (Sect. 8.6.1), the laser flash method has the advantage that the specimen under investigation does not need to be sandwiched between two surfaces. As a result, the interface between the specimen and an external surface is not involved in the laser flash method, but it is involved in the guarded hot plate method. This means that the work needed in the setup shown in Fig. 8.17 to decouple the contribution of the specimen to the thermal resistance from the contribution of the interface is not required when the laser flash method is used.

The thermal diffusivity describes the ease with which heat is transported by conduction in a material (i.e., the heat moves from one point to another within the material). Along the path of heat transport, the material is heated, thereby consuming heat; the amount consumed is governed by the volumetric specific heat. The higher the volumetric specific heat, the greater the heat consumed. The

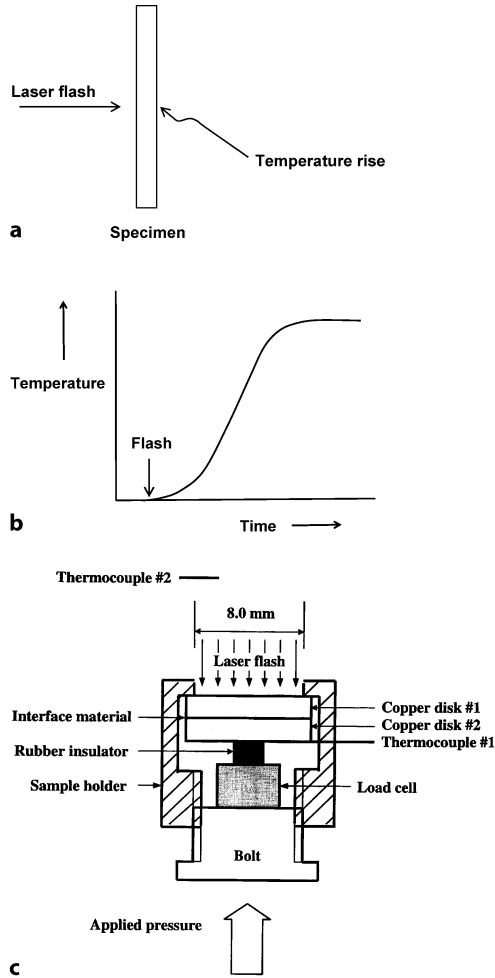


**Figure 8.19.** The laser flash method of evaluating thermal conduction. **a** Testing geometry, with the laser flash originating from the left. **b** Temperature rise at the back side of the specimen. **c** An example of a detailed experimental setup, with the laser flash originating from the top, thermocouple 2 for sensing the laser flash, and thermocouple 1 for measuring the temperature rise at the back of the specimen. The sample holder in this particular setup involves the use of a load cell to apply pressure to the specimen during testing. This particular configuration is used to evaluate thermal interface materials (Sect. 8.7)

more heat consumed, the less remains to reach the destination, and hence the lower the temperature rise at the destination and the lower the thermal diffusivity.

Table 8.5 lists the thermal diffusivity values of various materials. Pyrolytic graphite is a form of polycrystalline graphite that has a strong crystallographic texture, so the carbon layers are preferentially oriented in a plane. Due to the low density of pyrolytic graphite and its high thermal conductivity parallel to the carbon layers, pyrolytic graphite exhibits a very high thermal diffusivity parallel to the carbon layers. Its thermal diffusivity is even higher than those of silver and

**Table 8.5.** Thermal diffusivities of various materials

Material	Thermal diffusivity (m <sup>2</sup> /s)
Pyrolytic graphite (parallel to the carbon layers)	$1.22 \times 10^{-3}$
Silver	$1.6563 \times 10^{-4}$
Copper	$1.1234 \times 10^{-4}$
Air (1 atm, 300 K)	$2.2160 \times 10^{-5}$
Alumina	$1.20 \times 10^{-5}$
Pyrolytic graphite (perpendicular to the carbon layers)	$3.6 \times 10^{-6}$
Common brick	$5.2 \times 10^{-7}$
Window glass	$3.4 \times 10^{-7}$
Nylon	$9 \times 10^{-8}$

copper, which have higher thermal conductivities but also higher densities. The thermal diffusivity of air is higher than those of alumina and pyrolytic graphite (perpendicular to the carbon layers) because of the low density of air. Nylon has a very low thermal diffusivity because of its low thermal conductivity.

An example of a laser flash testing system is described below and illustrated in Fig. 8.19c. A Coherent General Everpulse Model 11 Nd (neodymium) glass laser (a solid-state laser) with a pulse duration of 0.4 ms, a wavelength of 1.06  $\mu\text{m}$  (near-infrared) and a pulse energy of up to 15 J is used for impulse heating. The laser power is adjusted to allow the temperature rise of the specimen to be between 0.5 and 1.0°C. The upper surface of disk #1, on which the laser beam impacts, is coated with carbon in order to increase the extent of laser energy absorption relative to the extent of reflection. An E-type thermocouple (#1) is attached to the back surface of disk #2 to monitor the temperature rise. Another thermocouple (#2) of the same type is put  $\sim 30$  cm above the specimen holder to detect the initial time when the laser beam is emitted. A plexiglass holder is used to facilitate the application of pressure, which is used to tighten the interface (between the proximate copper surfaces) under investigation. A load cell is used to measure the pressure. Calibration using a standard NBS 8426 graphite disc (thickness = 2.62 mm) is performed before testing each specimen in order to ensure measurement accuracy. The data acquisition rate used for each test is adjusted so that there are at least 100 temperature data points during the temperature rise.

The experimental error in these transient thermal contact conductance measurements consists of (i) random error due to experimental data scatter and (ii) systematic error that is mainly due to the lag in the thermocouple response and partly due to the method used to calculate the conductance from the temperature data. The higher the thermal contact conductance, the greater the error.

## 8.7 Thermal Interface Materials

Due to the miniaturization of microelectronics, the amount of heat generated per unit area has been increasing year by year. In order to dissipate this heat efficiently,

it is necessary to improve the thermal contacts within the microelectronic package. Without adequate thermal contacts, heat dissipation is hampered, in spite of the possible presence of heat sinks of high thermal conductivity.

A thermal interface material (TIM) is a material positioned at the interface between two surfaces for the purpose of enhancing the flow of heat from one surface to the other. For example, one surface is the heat spreader and the other surface is the heat sink (Fig. 8.20). As another example, one surface is the heat spreader and the other surface is the CPU of a computer (Fig. 8.20). Surfaces are never perfectly flat (Fig. 8.20), so air pockets are associated with the valleys in the surface topography. As air is thermally insulating, the displacement of the air by a TIM is crucial to improving the thermal interface. Thus, the conformability of the TIM is critical (Fig. 8.21).

TIMs are needed to improve thermal contacts. By placing a thermal interface material at the interface between two components across which heat must flow, the thermal contact between the two components is improved. An important market

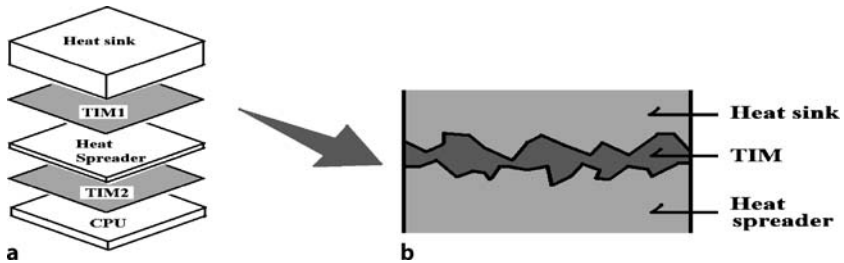


**Figure 8.20.** Schematic illustration of thermal interface materials (TIMs) sandwiched between two solid surfaces. **a** TIM1 at the interface between the heat sink and the heat spreader; TIM2 at the interface between the heat spreader and the CPU. **b** TIM filling the gap between two solid surfaces and conforming to the topography of the two surfaces

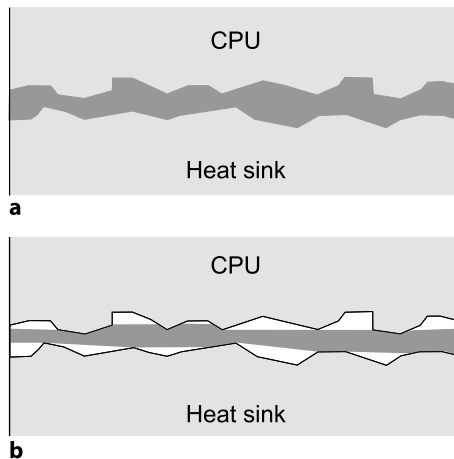


**Figure 8.21.** Schematic illustrations of thermal interface materials (TIMs, *dark regions*) with: **a** good conformability; **b** poor conformability. Poor conformability results in air pockets (*white regions*) at the thermal interface

for TIMs is the electronic industry, as heat dissipation is critical to the performance, reliability, and further miniaturization of microelectronics. For example, a TIM is used to improve the thermal contact between a heat sink and a printed circuit board, or between a heat sink and a chip carrier.

A TIM can be a thermal fluid, a thermal grease (paste), a resilient thermal conductor, or a solder applied in the molten state. The thermal fluid, thermal grease, or molten solder is spread on the mating surfaces. A resilient thermal conductor is sandwiched between the mating surfaces and held in place by pressure. The most commonly used thermal fluid is mineral oil, while the most commonly used thermal greases (pastes) are conducting particle (usually metal or metal oxide)-filled silicones. Conducting particle-filled elastomers are most commonly used as resilient thermal conductors. Among these four types of thermal interface materials, thermal greases (based on polymers, particularly silicone) and solder are by far the most commonly used. Resilient thermal conductors are not as well developed as thermal fluids or greases.

As the materials to be interfaced are good thermal conductors (such as copper), the effectiveness of a thermal interface material is enhanced if it has a high thermal conductivity and low thickness and if there is a low thermal contact resistance between the interface material and each mating surface. The rougher the mating surfaces, the larger the thickness required for the thermal interface material (Fig. 8.22). As the mating surfaces are not perfectly smooth, the interface material must be able to flow or deform in order to conform to the topographies of the mating surfaces. If the interface material is a fluid, grease, or paste, it should have a high fluidity (workability) in order to conform and to have a small thickness

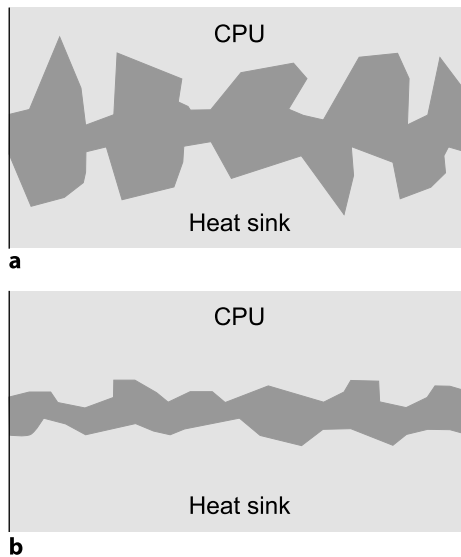


**Figure 8.22.** Thermal interface materials between: **a** rough surfaces; **b** smooth surfaces. Rough surfaces result in the need for large thicknesses of thermal interface material

after mating. On the other hand, the thermal conductivity of the grease or paste increases with increasing filler content, and this is accompanied by a decrease in the workability. Without a filler, as in the case of an oil, the thermal conductivity is poor. A thermal interface material in the form of a resilient thermal conductor sheet (e.g., a felt consisting of conducting fibers bound together without a binder, a resilient polymer-matrix composite containing a thermally conducting filler, and a form of graphite known as flexible graphite) cannot usually be as thin or conformable as one that takes the form of a fluid, grease, or paste, so it needs to have a very high thermal conductivity for it to be effective.

Solder is commonly used as a thermal interface material to enhance the thermal contact between two surfaces. This is because solder can melt at rather low temperatures and the molten solder can flow and spread itself thinly on the adjoining surfaces, thus resulting in high thermal contact conductance at the interface between the solder and each of the adjoining surfaces. Furthermore, solder in the metallic solid state is a good thermal conductor. In spite of the high thermal conductivity of solder, the thickness of the solder greatly affects the effectiveness of the solder as a thermal interface material; a small thickness is desirable. Moreover, the tendency for solder to react with copper to form intermetallic compounds reduces the thermal contact conductance of the solder-copper interface.

Thermal pastes are predominantly based on polymers, particularly silicone, although thermal pastes based on sodium silicate have been reported to be better at providing high thermal contact conductance. The superiority of sodium-silicate-based pastes over silicone-based pastes is primarily due to the low viscosity of sodium silicate compared to silicone, and the importance of high fluidity in the paste so that the paste can conform to the topography of the surfaces that it interfaces.

A TIM is generally prepared by combining an organic vehicle (liquid) or matrix (solid) with a thermally conductive filler, which typically takes the form of particles dispersed in the vehicle or matrix. When a vehicle is used, the TIM takes the form of a paste known as a thermal paste. A special type of matrix is a solid that melts upon heating at the operating temperature of the microelectronics. Such a matrix is known as a phase-change material, which is attractive due its lack of a tendency to seep during transportation, which occurs below the operating temperature. The vehicle or matrix should be able to conform to the topography of the proximate solid surfaces. In addition, it should be able to withstand the elevated temperatures present in the microelectronics package. Commonly used fillers are silver, boron nitride and zinc oxide particles, since they each exhibit high thermal conductivity and, in the case of boron nitride and zinc oxide, electrical nonconductivity, which is attractive for avoiding electrical short-circuiting in the microelectronic package upon the seepage of the thermal interface material.

Previously, the development of thermal interface materials has focused on maximizing the thermal conductivity of the interface material, with relatively little attention paid to the conformability. Thus, the volume fraction of the thermally conductive filler tends to be high in thermal interface materials, and the choice of filler has been governed by the thermal conductivity rather than the conformability of the filler.

Recent work by Chung et al. [1, 2] has shown that carbon black is a highly effective thermally conductive filler in thermal pastes, in spite of its moderate thermal conductivity. The effectiveness of carbon black is due to its conformability, which stems from the fact that carbon black takes the form of porous agglomerates of nanoparticles. Furthermore, Chung et al. [3] have shown that there is an optimum volume fraction of a filler, due to the increase in thermal conductivity and the decrease in conformability that occurs as the filler content increases. In addition, Chung et al. have shown that the performance of a TIM depends on the roughness of the proximate surfaces, with increasing demands being placed on the conformability as the roughness decreases and on the thermal conductivity as the roughness increases. Carbon black thermal paste, which shows excellent conformability, is particularly effective when the roughness is low.

The findings mentioned above have led to a paradigm shift in the design of TIMs [4]. The new criteria for designing a TIM are high conformability, low thickness (known as the bond line thickness, abbreviated to BLT, Fig. 8.23), and high thermal conductivity. A low thickness is important because the thermal resistance increases with increasing thickness. In order to achieve a low thickness, a TIM should be highly spreadable. Due to its conformability and spreadability, carbon black paste exhibits superior performance to both a single-walled carbon nanotube paste [5] and a carbon nanotube array [6]. The carbon nanotubes in the paste tend to lie down along the plane of the thermal interface and are also limited in terms of conformability. The carbon nanotube array has the nanotubes aligned in the direction of heat transfer, but it has a large thickness and the thermal conductivity of the array is limited.

This paradigm shift also means that the performance of a TIM cannot be described by the thermal conductivity of the TIM, but should instead be described by the thermal contact conductance between the two proximate surfaces. The thermal resistance of the overall thermal contact is the sum of the thermal resistance within the TIM and that of the interface between the TIM and each of the two proximate surfaces. The overall thermal resistance divided by the geometric area of the thermal contact gives the overall thermal resistivity. The reciprocal of the thermal resistivity is the thermal contact conductance (in  $W/(m^2 K)$ ). Performance comparisons for various TIMs must be conducted for the same composition and roughness of the proximate surfaces and for the same pressure that squeezes the two surfaces together. The guarded hot plate method (a steady-state method) can be used for this evaluation (Fig. 8.17). It is more reliable than the method of TIM



**Figure 8.23.** Schematic illustration of the bond line thickness (BLT) of a thermal interface material

performance evaluation that involves the measuring the temperature rise of an operating computer [7].

In the thermal pastes described below, unless noted otherwise, the vehicle consists of polyol esters. This is attractive due to its high workability and its ability to resist elevated temperatures. The polyol esters in the vehicle are a pentaerythritol ester of linear and branched fatty acids and a dipentaerythritol ester of linear and branched fatty acids. The polyol ester mixture is provided by Hatco Corp. (Fords, NJ, USA). The specific gravity is 0.97.

Carbon nanofillers that make effective thermal pastes have been studied comparatively [8]. These include carbon black (CB) and graphite nanoplatelets (GNPs, obtained by the sonication of exfoliated graphite). Figure 2.6 shows the nanoplatelet morphology of the GNPs. The GNPs have dimensions of around 3–8  $\mu\text{m}$  in the plane of the platelet. The platelet thickness is on the nanoscale. There are numerous types of carbon black that differ in terms of agglomerate size and particle size. Tokai black #3800 (graphitized carbon black from Tokai Carbon Co., Ltd., Tokyo, Japan) has a smaller structure (i.e., smaller agglomerates) and a smaller particle size than Vulcan XC72R carbon black (Cabot Corp., Billerica, MA, USA).

Table 8.6 and Fig. 8.24 show the thermal contact conductances of graphite nanoplatelet (GNP) pastes and carbon black (CB) pastes for both rough (15  $\mu\text{m}$ ) and smooth (0.01  $\mu\text{m}$ ) surfaces. For the rough surfaces, GNP is slightly more effective than CB (Tokai), which is in turn more effective than CB (Cabot). For the smooth surfaces, CB (Tokai) is more effective than CB (Cabot), which is in turn more effective than GNP. This comparison is based on testing various filler

**Table 8.6.** Thermal contact conductances of thermal contacts with graphite nanoplatelet (GNP) pastes and carbon black (CB) pastes. The bond line thicknesses of various pastes are shown in Fig. 8.24. (From [8])

Thermal paste		Thermal conductance ( $10^4 \text{ W}/(\text{m}^2 \text{ K})$ )				
Filler	Vol.%	Rough surfaces			Smooth surfaces	
		0.46 MPa	0.69 MPa	0.92 MPa	0.46 MPa	0.69 MPa
GNP	0.6	–	–	–	23.81 $\pm$ 0.34	25.18 $\pm$ 0.21
	1.2	10.66 $\pm$ 0.04	11.38 $\pm$ 0.05	11.66 $\pm$ 0.06	24.26 $\pm$ 0.66	25.66 $\pm$ 0.06
	2.4	11.72 $\pm$ 0.28	11.98 $\pm$ 0.18	12.36 $\pm$ 0.10	22.07 $\pm$ 1.18	24.47 $\pm$ 0.37
	3.6	10.32 $\pm$ 0.15	10.71 $\pm$ 0.05	11.17 $\pm$ 0.09	21.17 $\pm$ 0.07	22.16 $\pm$ 0.28
	4.8	9.35 $\pm$ 0.34	10.74 $\pm$ 0.32	9.68 $\pm$ 0.34	17.40 $\pm$ 0.37	19.14 $\pm$ 0.21
CB (Tokai)	1.2	9.45 $\pm$ 0.02	9.59 $\pm$ 0.09	9.89 $\pm$ 0.02	–	–
	2.4	10.20 $\pm$ 0.20	11.01 $\pm$ 0.05	11.87 $\pm$ 0.08	24.23 $\pm$ 0.17	27.75 $\pm$ 0.11
	4.8	10.12 $\pm$ 0.16	11.10 $\pm$ 0.10	11.59 $\pm$ 0.15	–	–
	8.0	10.85 $\pm$ 0.20	11.39 $\pm$ 0.10	11.64 $\pm$ 0.12	30.41 $\pm$ 0.47	32.75 $\pm$ 0.19
	12.0	11.06 $\pm$ 0.27	11.71 $\pm$ 0.12	12.57 $\pm$ 0.28	–	–
	15.0	11.27 $\pm$ 0.34	12.41 $\pm$ 0.22	13.18 $\pm$ 0.11	25.58 $\pm$ 0.35	27.86 $\pm$ 0.10
CB (Cabot)	20.0	9.34 $\pm$ 0.21	9.86 $\pm$ 0.11	11.11 $\pm$ 0.13	17.48 $\pm$ 0.17	22.33 $\pm$ 0.29
	1.2	8.50 $\pm$ 0.16	9.39 $\pm$ 0.11	10.36 $\pm$ 0.20	–	–
	2.4	8.72 $\pm$ 0.07	10.18 $\pm$ 0.20	11.12 $\pm$ 0.12	25.91 $\pm$ 0.16	27.75 $\pm$ 0.14
	4.8	8.45 $\pm$ 0.11	9.39 $\pm$ 0.15	10.58 $\pm$ 0.11	19.10 $\pm$ 0.20	21.33 $\pm$ 0.32
	8.0	7.96 $\pm$ 0.08	8.71 $\pm$ 0.10	8.78 $\pm$ 0.09	16.52 $\pm$ 0.61	18.17 $\pm$ 0.22
	12.0	2.05 $\pm$ 0.02	2.28 $\pm$ 0.03	2.49 $\pm$ 0.02	–	–

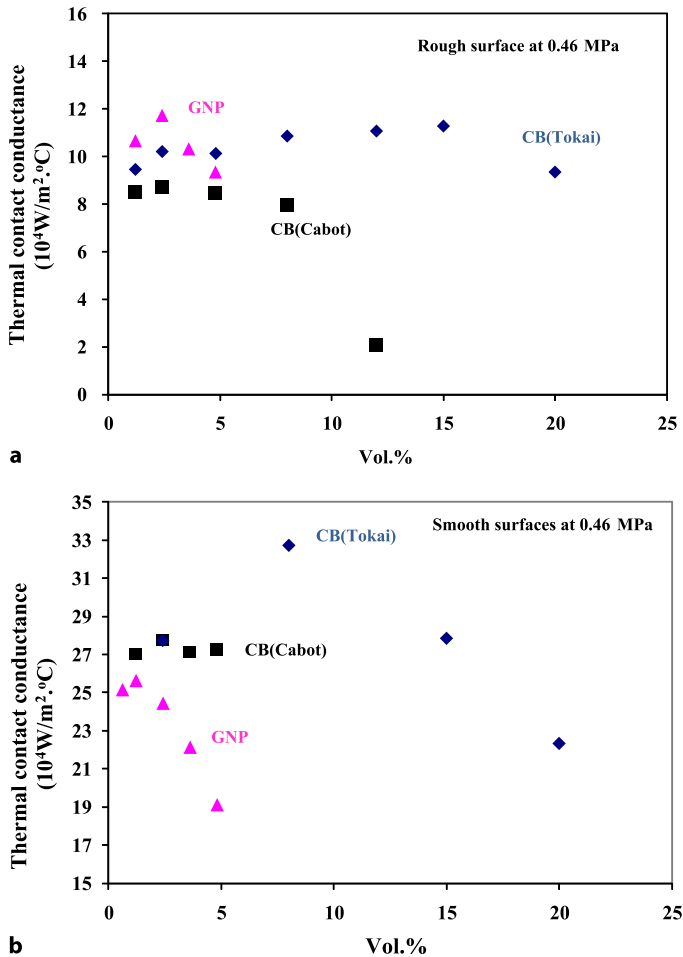


**Figure 8.24.** Thermal contact conductance measured for: **a** rough surfaces; **b** smooth surfaces. *Triangles*, GNP; *diamonds*, carbon black (Tokai); *squares*, carbon black (Cabot). A vertical bar with a horizontal line at each end indicating the data scatter is shown for each data point, though the bar is very short and thus covered by the data symbol for most data points

volume fractions for each type of filler and selecting the best performance. The highest value of thermal contact conductance attained for the rough surfaces is  $12 \times 10^4 \text{ W/m}^2 \text{ K}$  (as attained by GNP); the highest value of conductance attained for the smooth surfaces is  $33 \times 10^4 \text{ W/m}^2 \text{ K}$  (as attained by CB (Tokai)).

The high effectiveness of GNP for the rough surfaces is attributed to the high thermal conductivity of GNP. The high effectiveness of CB (Tokai) for the smooth surfaces is attributed to the high conformability, as suggested by its low viscosity [9]. Thermal conductivity is more important for rough surfaces than smooth surfaces, whereas conformability is more important for smooth surfaces than rough surfaces.

The optimum filler volume fraction differs among the three filler types. For the rough surfaces, the optimal fractions are 2.4, 15 and 2.4 vol% for GNP, CB (Tokai) and CB (Cabot), respectively. For the smooth surfaces, the optimal fractions are 1.2, 8 and 2.4 vol% for GNP, CB (Tokai) and CB (Cabot), respectively. Thus, the optimum filler volume fraction decreases as the proximate surfaces become smoother for GNP and CB (Tokai), but it is not affected by the surface smoothness for CB (Cabot). For GNP beyond the optimum volume fraction, the conductance decreases significantly with increasing GNP volume fraction (Fig. 8.24). Due to the low value of the optimum filler volume fraction for GNP compared to CB (Tokai), GNP is less effective than CB (Tokai) when the filler volume fraction exceeds about 5 vol% for rough surfaces. An optimum occurs because the thermal conductivity of the paste increases with increasing filler content while the conformability and spreadability of the paste decrease with increasing filler content. The optimal volume fraction is higher for rough surfaces than for smooth surfaces for the same filler type, as shown for both GNP and CB (Tokai), because of the relatively high importance of the thermal conductivity for rough surfaces and the relatively high importance of the conformability for smooth surfaces. The optimal volume fraction is higher for CB (Tokai) than for CB (Cabot) for both rough and smooth surfaces, and CB (Tokai) is more effective than CB (Cabot) for rough surfaces, because of the lower DBP value (i.e., the smaller structure) of CB (Tokai). Although the GNPs have nanoscale thicknesses, their other dimensions (in the plane of the platelet) are on the micron scale. The large in-plane dimensions and the expected tendency for the flakes to lie down in the plane of the thermal interface probably lead to the low optimum filler volume fraction of GNPs, akin to CB (Cabot), in the rough case.

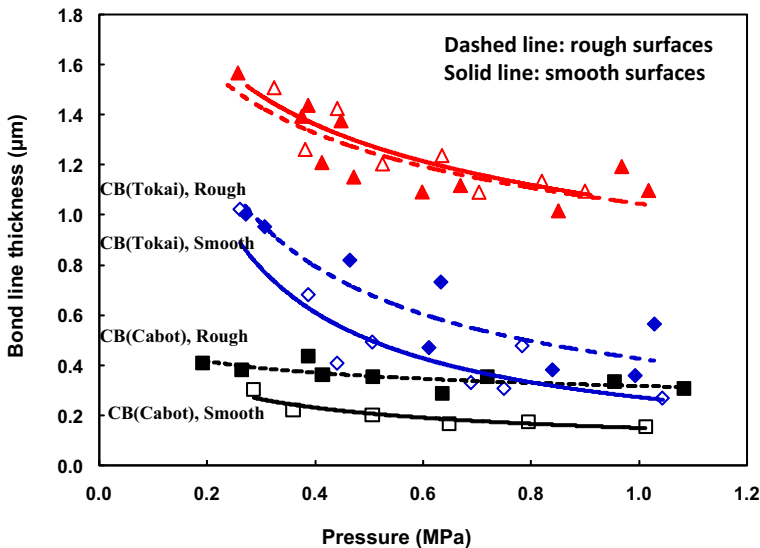


**Figure 8.25.** Bond line thicknesses for rough ( $15\ \mu\text{m}$ , *solid symbols*) and smooth ( $0.01\ \mu\text{m}$ , *open symbols*) proximate copper surfaces. *Triangles* – 2.4 vol% GNP pastes; *diamonds* – 15 vol% CB (Tokai); *squares* – 2.4 vol% CB (Cabot)

Figure 8.25 shows the dependence of the bond line thickness on the pressure for various thermal pastes and for rough (15  $\mu\text{m}$ ) and smooth (0.01  $\mu\text{m}$ ) proximate copper surfaces, respectively. For any paste, the bond line thickness decreases with increasing pressure, whether the proximate surfaces are rough or smooth. This trend is consistent with the increase in thermal contact conductance with increasing pressure, as observed for all of the pastes investigated, whether the proximate surfaces are rough or smooth (Table 8.6). This implies that the thermal contact conductance correlates with the bond line thickness for all of the pastes investigated.

As shown in Fig. 8.25, at the same pressure, 2.4 vol% GNP gives the highest bond line thickness, 2.4 vol % CB (Cabot) gives the lowest thickness, and 15 vol% CB (Tokai) gives an intermediate value, whether the proximate surfaces are rough or smooth. In particular, at a pressure of 0.46 MPa, which is one of the pressures used in the thermal contact conductance measurements, the bond line thicknesses are, respectively, 1.3, 0.72 and 0.36  $\mu\text{m}$  for 2.4 vol% GNP, 15 vol% CB (Tokai) and 2.4 vol% CB (Cabot) pastes in the case of rough surfaces.

Phase-change materials, which are solid at room temperature but melt at temperatures around the operating temperature, are attractive as thermal interface materials. This is because the phase change (melting) provides a mechanism of heat absorption and the molten state is associated with high fluidity. An example of a phase-change material is paraffin wax, which melts at 48°C. The addition of boron nitride particles to the wax makes the material effective as a thermal interface material; the thermal contact conductance (between copper, as in Table 8.6) reaches  $17 \times 10^4 \text{ W}/(\text{m}^2 \text{ K})$  at 22°C and 0.3 MPa.

Flexible graphite (a flexible foil that is all graphite) is effective as a thermal interface material if its thickness is low (0.13 mm), its density is low (1.1  $\text{g}/\text{cm}^3$ ) and the contact pressure used is high (11.1 MPa). It is much less effective than solder and thermal pastes, but flexible graphite is advantageous due to its thermal stability.

## 8.8 Composites Used for Microelectronic Heat Sinks

Materials of high thermal conductivity are needed to conduct heat for heating or cooling purposes, especially by the electronic industry. Due to the miniaturization and increasing power of microelectronics, heat dissipation is key to the reliability, performance, and further miniaturization of microelectronics. The heat dissipation problem is so severe that even expensive thermal conductors such as diamond, metal-matrix composites and carbon-matrix composites are being used in high-end microelectronics. Due to the low coefficients of thermal expansion (CTEs) of semiconductor chips and their substrates, heat sinks also need to have low CTEs. Thus, the thermal conductor material needs to have not just high thermal conductivity but low CTE too. For example, copper is a good thermal conductor but its CTE is high, as shown in Table 8.7. Therefore, copper-matrix composites containing low CTE fillers such as carbon fibers or molybdenum particles are used. For lightweight electronics, such as laptop computers and avionics, an additional requirement for

**Table 8.7.** Thermal properties and densities of various materials

Material	Thermal conductivity (W/(m K))	Coefficient of thermal expansion ( $10^{-6}^{\circ}\text{C}^{-1}$ )	Density ( $\text{g}/\text{cm}^3$ )
Aluminum	247	23	2.7
Gold	315	14	19.32
Copper	398	17	8.9
Lead	30	39	11
Molybdenum	142	4.9	10.22
Tungsten	155	4.5	19.3
Invar	10	1.6	8.05
Kovar	17	5.1	8.36
Diamond	2,000	0.9	3.51
Beryllium oxide	260	6	3
Aluminum nitride	320	4.5	3.3
Silicon carbide	270	3.7	3.3

the thermal conductor material is low density. As aluminum and carbon are light compared to copper, aluminum, carbon, and their composites are used for light purpose. Compared to aluminum, carbon has the additional advantage of being corrosion resistant.

### 8.8.1 Metals, Diamond, and Ceramics

Table 8.7 gives the thermal conductivities of various metals. Copper is most commonly used when materials of high thermal conductivity are required. However, copper suffers from a high coefficient of thermal expansion (CTE). A low CTE is needed when the adjoining component has a low CTE. When the CTEs of the two adjoining materials are sufficiently different and the temperature is varied, thermal stress occurs and may even cause warpage. This is the case when copper is used as heat sink for a printed wiring board, which is a continuous fiber polymer-matrix composite that has a lower CTE than copper. Molybdenum and tungsten are metals that have low CTEs, but their thermal conductivities are poor compared to copper. The alloy Invar (64Fe-36Ni) has an outstandingly low CTE among metals, but has a very poor thermal conductivity. Diamond is most attractive, as it has a very high thermal conductivity and a low CTE, but it is expensive. Aluminum is not as conductive as copper, but it has a low density, which is attractive for aircraft electronics and applications (e.g., laptop computers) that need to be light. Aluminum nitride is not as conductive as copper, but it is attractive due to its low CTE. Diamond and most ceramic materials are very different from metals in terms of their electrical insulation abilities. In contrast, metals conduct both thermally and electrically. For applications that require thermal conductivity and electrical insulation, diamond and appropriate ceramic materials can be used but metals cannot.

## 8.8.2 Metal-Matrix Composites

One way to lower the CTE of a metal is to form a metal-matrix composite using a low CTE filler. Ceramic particles such as AlN and SiC are used for this purpose, due to their combination of high thermal conductivity and low CTE. As the filler usually has a lower CTE and a lower thermal conductivity than the metal matrix, the higher the filler volume fraction in the composite, the lower the CTE and the lower the thermal conductivity.

Metal-matrix composites with discontinuous fillers (commonly particles) are attractive due to their high processability into various shapes. However, layered composites in the form of a matrix–filler–matrix sandwich are useful for planar components. Discontinuous fillers are most commonly ceramic particles. The filler sheets are most commonly low-CTE metal alloy sheets (e.g., Invar or 64Fe-36Ni, and Kovar or 54Fe-29Ni-17Co). Aluminum and copper are commonly used as metal matrices due to their high conductivities.

### 8.8.2.1 Aluminum-Matrix Composites

Aluminum is the most dominant matrix used in metal-matrix composites intended for both structural and electronic applications. This is because of the low cost of aluminum and its low melting point (660°C), which allows the composite to be fabricated by methods that involve melting the metal.

Liquid-phase methods used for the fabrication of metal-matrix composites include liquid metal infiltration, which usually involves the use of pressure (from a piston or compressed gas) to push the molten metal into the pores of a porous preform comprising the filler (commonly particles that are not sintered) and a small amount of a binder. Pressureless infiltration is less common but is possible. The binder prevents the filler particles from moving during the infiltration, and also provides sufficient compressive strength to the preform, so that the preform will not be deformed during the infiltration. This method thus provides near-net-shape fabrication; i.e., the shape and size of the composite product are the same as those of the preform. Since the composite is far more difficult to machine than the preform, near-net-shape fabrication is desirable.

In addition to the ability to perform near-net-shape fabrication, liquid metal fabrication is advantageous since it is able to provide composites with high filler volume fractions (up to 70%). A high filler volume fraction is necessary to attain a sufficiently low CTE ( $< 10 \times 10^{-6}/^{\circ}\text{C}$ ) in the composite, even if the filler is a low-CTE ceramic (e.g., SiC), since the aluminum matrix has a relatively high CTE. However, to attain a high volume fraction using liquid metal infiltration, the binder used must be present in only a small amount (to avoid clogging the pores in the preform) but still be effective. Hence, the binder technology used is critical.

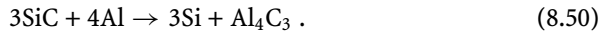
The ductility of a composite decreases as the filler volume fraction increases, so a composite with a low enough CTE is also quite brittle. Although this brittleness is not acceptable for structural applications, it is acceptable for electronic applications.

Another liquid-phase technique is stir casting, which involves stirring the filler in the molten metal and then casting. This method suffers from the nonuniform distribution of the filler in the composite due to the difference in density between the filler and the molten metal and the consequent tendency for the filler to either float or sink in the molten metal prior to solidification. Stir casting also suffers from an inability to produce composites with a high filler volume fraction.

Yet another liquid-phase technique is plasma spraying, which involves spraying a mixture of molten metal and filler onto a substrate. This method suffers from a relatively high porosity of the resulting composite and the consequent need for densification by hot isostatic pressing or other methods, which tend to be expensive.

One solid-phase technique is powder metallurgy, which involves mixing the matrix metal powder and filler and subsequent sintering under heat and pressure. This method is relatively difficult to use for an aluminum matrix because aluminum has a layer of protective oxide on it, and this oxide layer on the surface of each aluminum particle hinders sintering. Furthermore, this method is usually limited to low volume fractions of the filler.

The most common filler used is silicon carbide (SiC) particles, due to their low cost and the low CTE of SiC. However, SiC reacts with aluminum. The reaction is:



This reaction becomes more severe as the composite is heated. The aluminum carbide is a brittle reaction product that lines the filler–matrix interface of the composite, thus weakening the interface. Silicon, the other reaction product, dissolves in the aluminum matrix, lowering the melting temperature of the matrix, and causing nonuniform phase and mechanical property distributions. Furthermore, the reaction consumes some of the SiC filler.

One way to diminish this reaction is to use an Al-Si alloy matrix, since the silicon in the alloy matrix promotes the opposite reaction and thus counters this reaction. However, the Al-Si matrix is less ductile than the Al matrix, thus causing the mechanical properties of the Al-Si matrix composite to be far inferior to those of the corresponding Al-matrix composite. Thus, using an Al-Si alloy matrix is not a solution to the problem.

An effective solution is to replace SiC by aluminum nitride (AlN) particles, which do not react with aluminum, thus resulting in superior mechanical properties in the composite. The fact that AlN tends to have a higher thermal conductivity than SiC aids the thermal conductivity of the composite. Since the cost of the composite fabrication process is the biggest influence on the cost of composite production, the higher material cost of AlN compared to SiC does not matter, especially for electronic packaging. Aluminum oxide (Al<sub>2</sub>O<sub>3</sub>) also does not react with aluminum, but it does have a low thermal conductivity and it tends to suffer from particle agglomeration.

Other than ceramics such as SiC and AlN, another filler used in aluminum-matrix composites is carbon in the form of fibers with diameters of around 10 μm, and (less commonly) filaments (also known as nanofibers) with diameters of less than 1 μm.

Carbon also reacts with aluminum to form aluminum carbide. However, fibers are more effective than particles for reducing the CTE of the composite. Carbon fibers can even have continuous lengths. Moreover, carbon, especially when graphitized, is much more thermally conductive than ceramics. In fact, carbon fibers that are sufficiently graphitic are even more thermally conductive than the metal matrix, so the thermal conductivity of the composite increases with increasing fiber volume fraction. However, these fibers are expensive. The mesophase-pitch-based carbon fiber K-1100 (discontinued) from Amoco Performance Products (Alpharetta, GA, USA) exhibits a longitudinal thermal conductivity of 1,000 W/(m K).

Both carbon and SiC form galvanic couples with aluminum, which is the anode (the component in the composite that is corroded). The corrosion becomes more severe in the presence of heat and/or moisture.

The thermal conductivity of an aluminum-matrix composite depends on the filler and its volume fraction, the alloy matrix heat treatment condition, as well as the filler-matrix interface.

To increase the thermal conductivity of a SiC aluminum-matrix composite, diamond film can be deposited on the composite. The thermal conductivity of single-crystal diamond is 2,000–2,500 W/(m K), though diamond film is not single crystalline.

### **8.8.2.2 Copper-Matrix Composites**

Because copper is heavy anyway, the filler does not have to be lightweight. Thus, low-CTE but heavy metals such as tungsten, molybdenum and Invar are used as fillers. These metals (except Invar) have the advantage that they are quite conductive thermally and are available in particle and sheet forms, so that they are suitable for particulate as well as layered composites. Yet another advantage of the metal fillers is the better wettability of the molten matrix metal with metal fillers than with ceramic fillers when the composite is fabricated by a liquid phase method.

An advantage of copper over aluminum is its nonreactivity with carbon, so carbon is a highly suitable filler for copper. Additional advantages are that carbon is lightweight and carbon fibers are available in a continuous form. Furthermore, copper is a rather noble metal, as shown by its position in the electromotive series, so it does not suffer from the corrosion which plagues aluminum. Carbon is used as a filler in copper in the form of fibers with diameters of around 10  $\mu\text{m}$ . As carbon fibers that are sufficiently graphitic are even more thermally conductive than copper, the thermal conductivity of a copper-matrix composite can exceed that of copper. Less common fillers for copper are ceramics such as silicon carbide, titanium diboride ( $\text{TiB}_2$ ) and alumina.

The melting point of copper is much higher than that of aluminum, so copper-matrix composites are commonly fabricated by powder metallurgy, although liquid metal infiltration is also used. In the case of liquid metal infiltration, the metal matrix is often a copper alloy (e.g., Cu-Ag) chosen for its reduced melting temperature and good castability.

Powder metallurgy conventionally involves mixing the metal matrix powder and the filler, and then pressing and sintering under either heat or both heat and

pressure. The problem with this method is that it is limited to low volume fractions of the filler. In order to attain high volume fractions, a less conventional method of powder metallurgy is recommended. This method involves coating the matrix metal on the filler units, followed by pressing and sintering. The mixing of matrix metal powder with the coated filler is not necessary, although it can be done to decrease the filler volume fraction in the composite. The metal coating on the filler forces the distribution of matrix metal to be uniform even when the metal volume fraction is low (i.e., when the filler volume fraction is high). On the other hand, with the conventional method, the matrix metal distribution is not uniform when the filler volume fraction is high, thus causing porosity and the presence of filler agglomerates. In each of these agglomerates, the filler units touch one another directly. This microstructure results in low thermal conductivity and poor mechanical properties.

Continuous carbon fiber copper-matrix composites can be made by coating the fibers with copper and then diffusion bonding (i.e., sintering). This method is akin to the abovementioned less conventional method of powder metallurgy.

Less common fillers used in copper include diamond powder, aluminosilicate fibers and Ni-Ti alloy rod. The Ni-Ti alloy is attractive due to its negative CTE of  $-21 \times 10^{-6}/^{\circ}\text{C}$ .

Coatings can be used to further improve the thermal conductivity. This is particularly valuable when the substrate to be coated is prone to surface oxidation. The surface oxide tends to act as a thermal barrier. For example, a carbon fiber copper-matrix composite has been coated with a diamond film to enhance the thermal conductivity.

### 8.8.2.3 Beryllium-Matrix Composites

Beryllium oxide (BeO) has a high thermal conductivity (Table 8.4). Beryllium-matrix BeO-platelet composites with 20–60 vol% BeO exhibit low density (2.30 g/cm<sup>3</sup> at 40 vol% BeO, compared to 2.9 g/cm<sup>3</sup> for Al/SiC at 40 vol% SiC), high thermal conductivity (232 W/(m K) at 40 vol% BeO, compared to 130 W/(m K) for Al/SiC at 40 vol% SiC), low CTE ( $7.5 \times 10^{-6}/^{\circ}\text{C}$  at 40 vol% BeO, compared to  $12.1 \times 10^{-6}/^{\circ}\text{C}$  at 40 vol% SiC), and high modulus (317 GPa at 40 vol% BeO, compared to 134 GPa for Al/SiC at 40 vol% SiC).

## 8.8.3 Carbon-Matrix Composites

Carbon is an attractive matrix for composites used for thermal conduction because of its high thermal conductivity (though not as high as those of metals) and low CTE (lower than those of metals). Furthermore, carbon is corrosion resistant (more corrosion resistant than metals) and lightweight (lighter than metals). Yet another advantage of the carbon matrix is its compatibility with carbon fibers, in contrast to the common reactivity between a metal matrix and its fillers. Hence, carbon fibers are the dominant filler for carbon-matrix composites. Composites where both the filler and the matrix are carbon are called carbon-carbon composites. Their

primary applications in relation to thermal conduction are heat sinks, thermal planes and substrates. There is considerable competition between carbon-carbon composites and metal-matrix composites for the same applications.

The main drawback of carbon-matrix composites is their high cost of fabrication, which typically involves making a pitch-matrix or resin-matrix composite and subsequent carbonization (by heating at 1,000–1,500°C in an inert atmosphere) of the pitch or resin to form a carbon-matrix composite. After carbonization, the carbon matrix is relatively porous, so pitch or resin is impregnated into the composite and then carbonization is carried out again. Quite a few impregnation-carbonization cycles are needed in order to reduce the porosity to an acceptable level, thus resulting in a high cost of fabrication. Graphitization (by heating at 2,000–3,000°C in an inert atmosphere) may follow carbonization (typically in the last cycle) in order to increase the thermal conductivity, which increases with the degree of graphitization. However, graphitization is an expensive step. Some or all of the impregnation-carbonization cycles may be replaced by chemical vapor infiltration (CVI), in which a carbonaceous gas infiltrates the composite and decomposes to form carbon.

Carbon-carbon composites have been made using conventional carbon fibers with diameters of around 10  $\mu\text{m}$ , as well as carbon filaments (also known as carbon nanofibers) grown catalytically from carbonaceous gases and with diameters of less than 1  $\mu\text{m}$ . Using graphitized carbon fibers, thermal conductivities exceeding that of copper can be reached.

Carbon-carbon composites are typically less conductive than copper. To increase the thermal conductivity, carbon-carbon composites can be impregnated with copper and can also be coated with a diamond film.

#### 8.8.4 Carbon and Graphite

An all-carbon material (called ThermalGraph, a tradename of Amoco Performance Products, Alpharetta, GA, USA), made by consolidating oriented precursor carbon fibers without a binder and subsequent carbonization and optional graphitization, exhibits thermal conductivities ranging from 390 to 750 W/(m K) in the fiber direction of the material.

Another material is pyrolytic graphite (called TPG) encased in a structural shell. The graphite (highly textured with the *c*-axes of the grains preferentially perpendicular to the plane of the graphite), has an in-plane thermal conductivity of 1,700 W/(m K) (four times that of copper), but it is mechanically weak due to the tendency to shear in the plane of the graphite. The structural shell serves to strengthen by hindering shear.

Pitch-derived carbon foams with thermal conductivities of up to 150 W/(m K) after graphitization are attractive due to their high specific thermal conductivities (thermal conductivity divided by the density).

### 8.8.5 Ceramic-Matrix Composites

The SiC matrix is attractive due to its high CTE compared to the carbon matrix, though it is not as thermally conductive as carbon. The CTE of carbon-carbon composites is too low ( $0.25 \times 10^{-6}/^{\circ}\text{C}$ ), thus resulting in reduced fatigue life in chip-on-board (COB) applications with silica chips ( $\text{CTE} = 2.6 \times 10^{-6}/^{\circ}\text{C}$ ). The SiC-matrix carbon fiber composite is made from a carbon-carbon composite by converting the matrix from carbon to SiC. To improve the thermal conductivity of the SiC-matrix composite, coatings in the form of chemical vapor deposited AlN or Si have been used. The SiC-matrix metal (Al or Al-Si) composite, as made by a liquid-exchange process, also exhibits relatively high thermal conductivity.

The borosilicate glass matrix is attractive due to its low dielectric constant (4.1 at 1 MHz for  $\text{B}_2\text{O}_3\text{-SiO}_2\text{-Al}_2\text{O}_3\text{-Na}_2\text{O}$  glass), compared to 8.9 for AlN, 9.4 for alumina (90%), 42 for SiC, 6.8 for BeO, 7.1 for cubic boron nitride, 5.6 for diamond and 5.0 for glass-ceramic. A low value of the dielectric constant is desirable for electronic packaging applications. On the other hand, glass has a low thermal conductivity. Hence, fillers with relatively high thermal conductivity are used with the glass matrix. An example is continuous SiC fibers, the glass-matrix composites of which are made by tape casting followed by sintering. Another example is aluminum nitride with interconnected pores (about 28 vol%), the composites of which are obtained by glass infiltration to a depth of about 100  $\mu\text{m}$ .

### 8.8.6 Polymer-Matrix Composites

Polymer-matrix composites with continuous or discontinuous fillers are used for thermal management. Composites with continuous fillers (fibers, whether woven or not) are used as substrates, heat sinks, and enclosures. Composites with discontinuous fillers (particle or fibers) are used for die (semiconductor chip) attachment, electrically/thermally conducting adhesives, encapsulations, and thermal interface materials. Composites with discontinuous fillers can be in a paste form during processing, thus allowing their application by printing (screen printing or jet printing) and injection molding. Composites with continuous fillers cannot undergo paste processing, but the continuous fillers provide lower thermal expansion and higher conductivity than discontinuous fillers.

Composites can have thermoplastic or thermosetting matrices. Thermoplastic matrices have the advantage that a connection can be reworked by heating for repair purposes, whereas thermosetting matrices do not allow reworking. On the other hand, controlled-order thermosets are attractive for their thermal stability and dielectric properties. Polymers exhibiting a low dielectric constant, low dissipation factor, low coefficient of thermal expansion, and compliance are preferred.

Composites can be electrically conducting or electrically insulating; the electrical conductivity is provided by a conductive filler. The composites can be made both electrically and thermally conducting through the use of metal or graphite fillers; they can also be made electrically insulating but thermally conducting through the use of diamond, aluminum nitride, boron nitride, or alumina fillers. An electrically

conducting composite can be isotropically conducting or anisotropically conducting. A  $z$ -axis conductor is an example of an anisotropic conductor; it is a film that is electrically conducting only along the  $z$ -axis (i.e., in the direction perpendicular to the plane of the film). As one  $z$ -axis film can replace a whole array of solder joints,  $z$ -axis films are valuable for solder replacement, reducing processing costs, and improving repairability.

Epoxy-matrix composites that have continuous glass fibers and are made by lamination are most commonly used for printed wiring boards, due to the electrically insulating nature of glass fibers and the good adhesive behavior and established industrial usage of epoxy. Aramid (Kevlar) fibers can be used instead of glass fibers to provide a lower dielectric constant. Alumina ( $\text{Al}_2\text{O}_3$ ) fibers can be used to increase the thermal conductivity. By selecting the fiber orientation and loading in the composite, the dielectric constant can be decreased and the thermal conductivity can be increased. By impregnating the yarns or fabrics with a silica-based sol and subsequent firing, the thermal expansion can be reduced. Matrices other than epoxy can be used. Examples are polyimide and cyanate ester.

For heat sinks and enclosures, conducting fibers are used, since the conducting fibers enhance the thermal conductivity and the ability to shield electromagnetic interference (EMI); i.e., to block electromagnetic radiation that is mainly in the radio wave frequency range. EMI shielding is particularly important for enclosures. Carbon fibers are most commonly used for these applications due to their conductivity, low thermal expansion, and wide availability as a structural reinforcement. For high thermal conductivity, carbon fibers made from mesophase pitch or copper-plated carbon fibers are preferred.

## 8.9 Carbon Fiber Polymer-Matrix Composites for Aircraft Heat Dissipation

Heat dissipation from aircraft systems is increasingly important due to the rapid increase in thermal load, which is expected to reach 10,000 kW. The increased thermal load is a consequence of the limited aircraft idling time, the heating of the fuel by electronics, increased engine performance, increased flight speed, and the heat generated by high-energy lasers. Furthermore, low temperatures are required for the reliability of electron field emitters (cold cathodes).

Polymer-matrix composites with continuous and aligned carbon fiber reinforcement are widely used for lightweight structures, due to their high strength-to-weight ratio, good fatigue resistance, and corrosion resistance. They are increasingly used in both commercial and military aircraft. Although the polymer matrix is not conductive, the carbon fibers in the composite give it a high in-plane thermal conductivity. Carbon fibers that are even more conductive thermally than copper are commercially available. The high in-plane thermal conductivity promotes heat spreading. However, a drawback of these composites is the low through-thickness thermal conductivity, which hinders heat removal in the through-thickness direction (the direction perpendicular to the laminae). Both in-plane heat spreading and through-thickness heat removal are important for effective heat dissipation.

Methods for increasing the through-thickness thermal conductivity of polymer-matrix composites include the use of continuous carbon fiber with carbon nanofibers grown on its surface and the use of continuous silicon carbide fiber with aligned carbon nanotubes grown perpendicular to its surface. The nanofibers or nanotubes promote heat conduction in the through-thickness direction. In the case of silicon carbide fibers, the carbon nanotubes grown on the fibers increase the through-thickness thermal conductivity of the epoxy-matrix composite by 50% and increase the flexural modulus by 5%. However, the presence of nanofibers or nanotubes results in a low fiber volume fraction in the composite, thus limiting the reinforcing ability. In addition, such modified continuous fibers make composite fabrication difficult and costly.

A particularly effective and practical method for increasing the thermal conductivity of a carbon fiber polymer-matrix composite in the through-thickness direction involves interlaminar interface nanostructuring. As this interface is the polymer-rich region between adjacent laminae, it contributes significantly to the thermal resistance of the composite in the through-thickness direction. Improving the thermal contact across the interlaminar interface allows the through-thickness thermal conductivity of the composite to be increased.

Although polymer-matrix composites with continuous carbon fiber exhibit excellent tensile properties in the fiber direction (in the plane of the laminae in the case of a multidirectional composite), the weak link at the interlaminar interface causes the through-thickness compressive properties to be poor. The poor through-thickness compressive properties are of concern to the quality and durability of composite joints made by fastening, which involves the application of a through-thickness compressive stress. This concern is relevant to aircraft safety, as indicated by the 2001 Airbus accident in New York. The accident involved detachment of the tail section from the body of the aircraft (Investigation of the Crash of American Airlines Flight 587; <http://www.airsafe.com/events/aa587.htm>). Increasing the through-thickness compressive modulus can also be achieved by nanostructuring the interlaminar interface.

A composite panel commonly encounters flexural loading. The weak link at the interlaminar interface is a disadvantage with respect to the flexural properties. The flexural modulus can also be increased by nanostructuring the interlaminar interface.

### **8.9.1 Interlaminar Interface Nanostructuring**

The interlaminar interface nanostructuring involves the application of conductive nanoparticles between the laminae during the fabrication of the composite, such that the nanoparticles fit between the fibers of the adjacent laminae without causing the fibers of the adjacent laminae to move farther away from one another. Carbon nanoparticles in the form of carbon black are inexpensive and ineffective. The vehicle (liquid carrier) used to disperse the carbon black is chosen so as to remove part of the resin on the surface of the carbon fiber epoxy prepreg. Both the removal of the partial resin and the addition of the carbon black contribute to improving the thermal contact across the interlaminar interface.

The effect of the interlaminar interface nanostructuring depends on the relative orientations of the fibers on the two sides of the interlaminar interface. When the fibers of the two laminae are not parallel, the fibers of one lamina tend to press against those of the adjacent lamina, thus resulting in substantial fiber–fiber contact across the interlaminar interface (as indicated by a relatively low value of the electrical contact resistivity of the interface). On the other hand, when the fibers of the two laminae are parallel, the fibers of one lamina tend to sink into the adjacent laminae to a certain degree, thus resulting in relatively little fiber–fiber contact across the interlaminar interface (as indicated by a relatively high value of the contact resistivity of the interface). In practice, structural composites are not unidirectional but involve fibers of different orientations in the various laminae in the composite. The crossply configuration may be used to represent the general situation in which the fibers of the two adjacent laminae are not parallel.

### 8.9.2 Through-Thickness Thermal Conductivity

As shown in Figs. 8.28 and 6.13 for unidirectional and crossply composites, respectively, the thermal conductivity is enhanced by using the vehicle ethylene glycol monoethyl ether (EGME) without carbon black for interlaminar interface modification and is further increased by using the vehicle with carbon black. The optimal carbon black content for attaining the highest thermal conductivity is 0.8 wt.% (with respect to the vehicle). The trend is the same for unidirectional and crossply configurations, but the thermal conductivity is higher for the crossply configuration than for the unidirectional configuration in every case except for the highest carbon black content of 1.2 wt.%. At the optimal carbon black content of 0.8 wt.%, the thermal conductivity increases (relative to the case of no interlaminar interface modification) are 115 and 212% for unidirectional and crossply

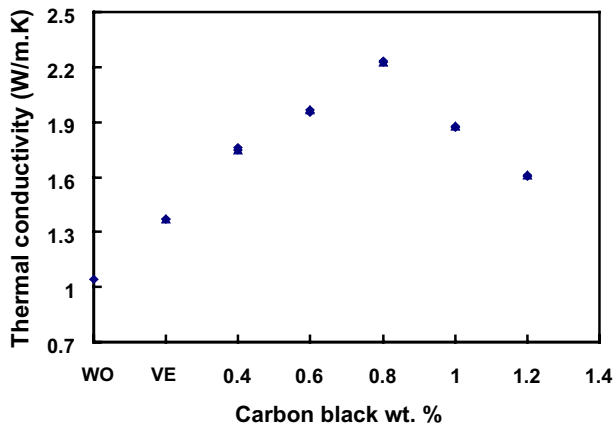


**Figure 8.26.** Thermal conductivities of unidirectional carbon fiber polymer-matrix composites with and without various interlaminar interface modifications. WO – without carbon black and without vehicle. VE – with vehicle and without carbon black. Three specimens of each composition were tested

configurations, respectively. In contrast, the fractional increase attained by using aligned carbon nanotubes grown on continuous silicon carbide fibers is only 50%.

Although both the vehicle and the carbon black are useful for improving the through-thickness thermal conductivity, the effect of carbon black is greater than that of EGME, as shown by the much larger fractional increase in thermal conductivity relative to the unmodified composite when both carbon black and vehicle are used than when only EGME is used, whether the configuration is unidirectional or crossply.

The observation that the thermal conductivity is increased by the use of EGME without carbon black is consistent with the fact that the vehicle dissolves away part of the resin at the interface, thereby allowing greater proximity between the fibers of the adjacent laminae. The observation that the thermal conductivity is further increased by the use of EGME with carbon black is consistent with the fact that the carbon black is a conformable and conductive filler that improves the thermal contact across the interlaminar interface. The fact that an excessive content of carbon black decreases the thermal conductivity relative to the value at the optimal carbon black content is due to the separation of the fibers of the adjacent laminae when the carbon black content is excessive. The thermal conductivity is higher for the crossply configuration than the unidirectional configuration because of the larger number of fiber–fiber contacts across the interlaminar interface for the crossply configuration.

### 8.9.3 Through-Thickness Compressive Properties

Figures 8.27 and 8.28 show the through-thickness compressive moduli, as determined from the slope of the compressive stress–strain curve in the elastic regime, for unidirectional and crossply composites, respectively. The modulus is decreased

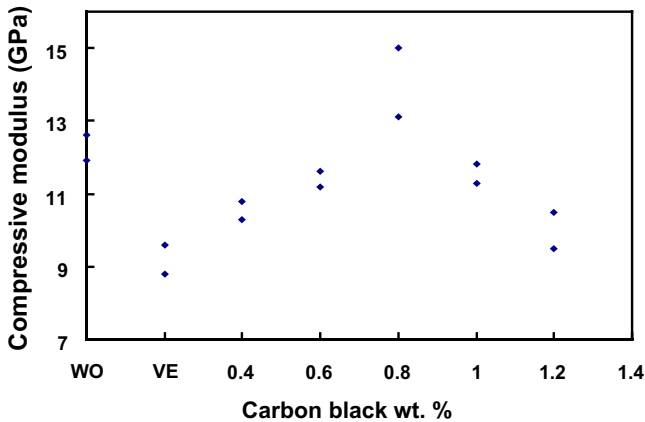


**Figure 8.27.** Through-thickness compressive moduli of unidirectional carbon fiber polymer-matrix composites with and without various interlaminar interface modifications. WO – without carbon black and without vehicle. VE – with vehicle and without carbon black. Two specimens of each composition were tested

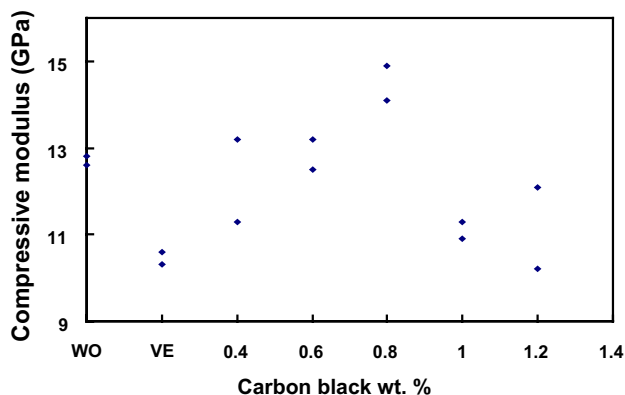


**Figure 8.28.** Through-thickness compressive moduli of crossply carbon fiber polymer-matrix composites with and without various interlaminar interface modifications. WO – without carbon black + without vehicle. VE – with vehicle + without carbon black. Two specimens of each composition were tested

by the use of the vehicle in the absence of carbon black, such that the decrease is more significant for the unidirectional composite than the crossply composite. This difference between unidirectional and crossply composites is attributed to the negligible thickness of the interlaminar interface for the unidirectional composite and the observable thickness of the interface for the crossply composite. However, the combined use of EGME and carbon black causes the modulus to increase from the value for modification with EGME alone. The optimal carbon black content in EGME that achieves the highest value of the modulus is 0.8 wt.% , whether the composite is unidirectional or crossply. Beyond this optimal value, the modulus decreases, due to the excessive thickness of the interlaminar interface. When EGME contains the optimal amount of carbon black, the modulus exceeds that of the unmodified composite by up to 14% and exceeds that of the composite modified with the vehicle alone by up to 52%. The fractional increase of the modulus relative to the corresponding unmodified composite is similar for the unidirectional and crossply composites.

The nanostructuring improves the through-thickness compressive strength (data not included here) for the crossply composites, and has a negligible effect on the unidirectional composites. This observation supports the quality of the nanostructured composites.

### 8.9.4 Flexural Properties

Figures 8.29 and 8.30 show values of the flexural modulus (three-point bending) for unidirectional and crossply composites, respectively. For each formulation, the flexural modulus is higher for the unidirectional composite than the crossply composite. This is because the 90° fiber of the crossply composite does not contribute to the flexural stiffness. The modulus is essentially unaffected by the use of EGME in the absence of carbon black. However, the combined use of EGME and carbon black

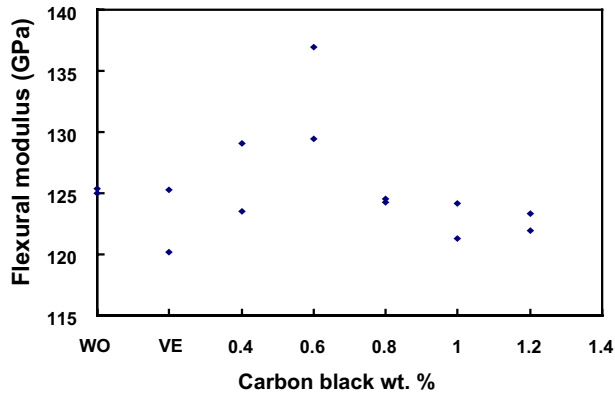


**Figure 8.29.** Flexural moduli of unidirectional carbon fiber polymer-matrix composites with and without various interlaminar interface modifications. WO – without carbon black + without vehicle. VE – with vehicle + without carbon black. Two specimens of each composition were tested

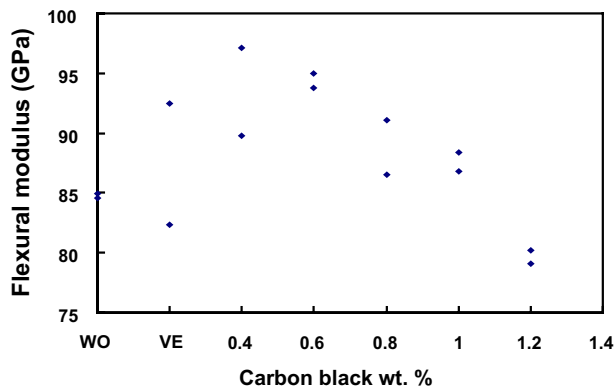


**Figure 8.30.** Flexural moduli of crossply carbon fiber polymer-matrix composites with and without various interlaminar interface modifications. WO – without carbon black + without vehicle. VE – with vehicle + without carbon black. Two specimens of each composition were tested

causes the modulus to increase from the value for modification with the vehicle alone. The optimal carbon black content in EGME that achieves the highest value of the modulus is 0.6 wt.%, whether the composite is unidirectional or crossply. (In the crossply case, the optimum is either 0.4 or 0.6 wt.%) Beyond the optimal value, the modulus decreases due to the excessive thickness of the interlaminar interface. When the vehicle contains the optimal amount of carbon black, the modulus exceeds that of the corresponding unmodified composite by up to 6 and 11% for the unidirectional and crossply composites, respectively, and exceeds that of the corresponding composite modified with the vehicle alone by up to 9 and 8% for unidirectional and crossply composites, respectively. The fractional increase in the modulus, whether it is relative to the corresponding unmodified composite or relative to the composite modified by using the vehicle alone, is comparable for

the crossply and unidirectional composites. This occurs in spite of the fact that the  $90^\circ$  fiber of the crossply composite does not contribute to the flexural stiffness and the interlaminar interface is between  $0$  and  $90^\circ$  laminae. It is probably partly due to the tendency for the  $0$  and  $90^\circ$  fibers in the crossply composite to press onto one another during flexure, thus increasing the importance of the interlaminar interface.

The effect of the interlaminar interface modification on the flexural modulus is less than that on the through-thickness compressive modulus, particularly when the composite is unidirectional. For example, for the unidirectional configuration, the fractional increase in through-thickness compressive modulus relative to the unmodified composite is up to 14%, whereas the fractional increase in flexural modulus relative to the unmodified composite is up to 6%. Although the improvement in the flexural modulus is small, it is important that the optimum interlaminar interface modification does not degrade the flexural modulus. In contrast, the fractional increase attained by using aligned carbon nanotubes grown on continuous silicon carbide fibers is only 5%.

The effect of the nanostructuring on the flexural strength (data not included here) is negligible for both crossply and unidirectional composites. This observation supports the quality of the nanostructured composites.

## 8.10 Composites Used for Thermal Insulation

Materials used for thermal insulation are characterized by a low thermal conductivity (Table 8.4), which is most commonly attained by the use of air (a thermal insulator), as in the case of polymer foams (e.g., Styrofoam, which is a trademark of the Dow Chemical Company for extruded polystyrene foam), glass fiber felts, and porous ceramics (e.g., perlite and vermiculite). Perlite is an amorphous volcanic glass that expands upon heating, due to the vaporization of the trapped water. Vermiculite is a natural clay mineral that expands upon heating. Foaming agents may be used in the fabrication of polymer and cement materials in order to provide a large number of small air cells that are uniformly distributed. Silica fiber tiles are used as a high-temperature thermal insulation for the Space Shuttles, which face very high temperatures during re-entry through the atmosphere. Multiple glass panes that are hermetically sealed (airtight) so that the environment inside the unit is isolated from that outside the unit are commonly used for insulated glass windows.

Composite materials for thermal insulation are designed to obtain a low thermal conductivity while the mechanical properties remain acceptable. They are mainly polymer-matrix and cement-matrix composites. Either type of composite typically contains a foamy or porous phase, which can be the matrix or the filler. However, such a phase is detrimental to the mechanical properties. For example, perlite and vermiculite are used as admixtures to decrease the thermal conductivity of concrete, although they decrease the strength of the concrete.

The use of a structural material that is itself a thermal insulator contrasts with the combined use of a structural material (which is not a thermal insulator) and

**Table 8.8.** Thermal conductivities and specific heats of cement-matrix composites in the form of cement pastes (from [10])

Cement paste	Thermal conductivity (W/(m K)) ( $\pm 0.03$ )	Specific heat (J/(g K)) ( $\pm 0.001$ )
Plain	0.52	0.703
+ latex (20% by mass of cement)	0.38	0.712
+ latex (25% by mass of cement)	0.32	0.723
+ latex (30% by mass of cement)	0.28	0.736
+ methylcellulose (0.4% by mass of cement)	0.42	0.732
+ methylcellulose (0.6% by mass of cement)	0.38	0.737
+ methylcellulose (0.8% by mass of cement)	0.32	0.742
+ silica fume	0.36	0.765
+ silica fume + methylcellulose <sup>a</sup>	0.33	0.771
+ methylcellulose <sup>a</sup> + fibers <sup>b</sup> (0.5% by mass of cement)	0.44	0.761
+ methylcellulose <sup>a</sup> + fibers <sup>b</sup> (1.0% by mass of cement)	0.34	0.792
+ silica fume + methylcellulose <sup>a</sup> + fibers <sup>b</sup> (0.5% by mass of cement)	0.28	0.789

<sup>a</sup> 0.4% by mass of cement; <sup>b</sup> carbon fibers

a thermal insulator (which is not a structural material). The former is attractive due to the space saved and the durability of the structural material. However, the development of a structural material that is also a thermal insulator is scientifically challenging. One route is to use the interfaces rather than pores in the structural composite (such as the filler–matrix interface, with the filler being either particles or fibers) to provide thermal barriers.

In the case of a cement-matrix composite, methods of decreasing the thermal conductivity involve (i) the addition of a polymer (e.g., latex particles) admixture, since the thermal conductivity of a polymer is lower than that of cement, and (ii) the use of interfaces as thermal barriers. Table 8.8 lists the thermal conductivities of various cement pastes that utilize silica fume (fine particles), latex (a polymer), methylcellulose (molecules) and short carbon fibers as admixtures. Although carbon fibers are thermally conducting, the addition of carbon fibers to cement lowers the thermal conductivity, thus allowing applications related to thermal insulation. This effect of carbon fiber addition occurs due to the increase in air void content. The electrical conductivity of carbon fibers is higher than that of the cement matrix by about eight orders of magnitude, whereas the thermal conductivity of carbon fibers is higher than that of the cement matrix by only one or two orders of magnitude. As a result, the electrical conductivity increases upon carbon fiber addition in spite of the increase in air void content, but the thermal conductivity decreases upon fiber addition.

## Example Problems

1. Calculate the thermal expansion coefficient of a composite material that consists of three components in series (Fig. 8.2a). Component 1 has a CTE of  $4.1 \times 10^{-6}/^{\circ}\text{C}$  and a volume fraction of 0.29. Component 2 has a CTE of  $6.7 \times 10^{-5}/^{\circ}\text{C}$  and a volume fraction of 0.21. Component 3 has a CTE of  $7.8 \times 10^{-6}/^{\circ}\text{C}$  and a volume fraction of 0.50.

*Solution:*

From Eq. 8.8,

CTE of composite

$$\begin{aligned} &= [(0.29)(4.1 \times 10^{-6}) + (0.21)(6.7 \times 10^{-5}) + (0.50)(7.8 \times 10^{-6})]/^{\circ}\text{C} \\ &= 1.9 \times 10^{-5}/^{\circ}\text{C} \end{aligned}$$

2. Derive an expression for the thermal expansion coefficient of a composite material that consists of three components in parallel (Fig. 8.2b). Assume perfect bonding between the components. Component 1 has a CTE of  $\alpha_1$  and a volume fraction of  $v_1$ . Component 2 has a CTE of  $\alpha_2$  and a volume fraction of  $v_2$ . Component 3 has a CTE of  $\alpha_2$  and a volume fraction of  $v_3$ .

*Solution:*

Since there is no applied force,

$$F_1 + F_2 + F_3 = 0 ,$$

where  $F_1$ ,  $F_2$ , and  $F_3$  are the thermal forces in components 1, 2, and 3 respectively. Hence,

$$(\alpha_c - \alpha_1)M_1v_1 + (\alpha_c - \alpha_2)M_2v_2 + (\alpha_c - \alpha_3)M_3v_3 = 0 .$$

Rearrangement gives

$$\alpha_c = (\alpha_1M_1v_1 + \alpha_2M_2v_2 + \alpha_3M_3v_3)/(M_1v_1 + M_2v_2 + M_3v_3) .$$

3. Calculate the thermal conductivity of a composite material that consists of three components in parallel. The conductivity is in the parallel direction. Component 1 has a thermal conductivity of  $3.8 \text{ W}/(\text{m K})$  and a volume fraction of 0.33. Component 2 has a thermal conductivity of  $2.1 \text{ W}/(\text{m K})$  and a volume fraction of 0.19. Component 3 has a thermal conductivity of  $4.1 \text{ W}/(\text{m K})$  and a volume fraction of 0.48.

*Solution:*

From Eq. 8.25,

$$\begin{aligned} \text{Thermal conductivity} &= [(0.33)(3.8) + (0.19)(2.1) + (0.48)(4.1)]\text{W}/(\text{m K}) \\ &= 3.6 \text{ W}/(\text{m K}) . \end{aligned}$$

4. Calculate the thermal conductance of an interface that consists of three components that are two-dimensionally distributed. The conductance is in the direction perpendicular to the interface. Component 1 has a thermal conductance of  $2.7 \times 10^4 \text{ W}/(\text{m}^2 \text{ K})$  and an area fraction of 0.61. Component 2 has a thermal conductance of  $8.9 \times 10^4 \text{ W}/(\text{m}^2 \text{ K})$  and an area fraction of 0.22. Component 3 has a thermal conductance of  $1.3 \times 10^4 \text{ W}/(\text{m}^2 \text{ K})$  and an area fraction of 0.39.

*Solution:* From Eq. 8.41,

$$\begin{aligned} \text{Thermal conductance} &= [(0.61)(2.7) + (0.22)(8.9) + (0.39)(1.3)] \\ &\quad \times 10^4 \text{ W}/(\text{m}^2 \text{ K}) \\ &= 4.1 \times 10^4 \text{ W}/(\text{m}^2 \text{ K}) . \end{aligned}$$

5. Calculate the specific heat of a composite material that consists of three components. Component 1 has a specific heat of  $1.52 \text{ J g}^{-1} \text{ K}^{-1}$  and a volume fraction of 0.68. Component 2 has a specific heat of  $0.34 \text{ J g}^{-1} \text{ K}^{-1}$  and a volume fraction of 0.21. Component 1 has a specific heat of  $3.81 \text{ J g}^{-1} \text{ K}^{-1}$  and a volume fraction of 0.11.

*Solution:* From Eq. 8.20,

$$\begin{aligned} \text{Specific heat} &= [(0.68)(1.52) + (0.21)(0.34) + (0.11)(3.81)] \text{ J g}^{-1} \text{ K}^{-1} \\ &= 1.5 \text{ J g}^{-1} \text{ K}^{-1} . \end{aligned}$$

6. Calculate the thermal conductivity of a metal that exhibits an electrical resistivity of  $1.5 \times 10^{-5} \Omega \text{ cm}$  at a temperature of  $450^\circ\text{C}$ .

*Solution:* From Eq. 8.33,

$$\begin{aligned} \text{Thermal conductivity} &= LT(\text{electrical conductivity}) \\ &= LT/(\text{electrical resistivity}) \\ &= (2.44 \times 10^{-8} \text{ W } \Omega/\text{K}^2)(450 + 273)\text{K}/(1.5 \times 10^{-5} \omega \text{ cm}) \\ &= 1.2 \times 10^2 \text{ W}/(\text{m K}) . \end{aligned}$$

7. Calculate the heat flow in a material that exhibits a thermal conductivity of  $46 \text{ W}/(\text{m K})$  under a temperature gradient of  $125^\circ\text{C}/\text{cm}$ . The cross-sectional area of the material is  $158 \text{ mm}^2$ .

*Solution:* From Eq. 8.22,

$$\text{Heat flow} = (46 \text{ W}/(\text{m K}))(158 \text{ mm}^2)(125^\circ\text{C}/\text{cm}) = 91 \text{ W} .$$

## Review Questions



1. Why is diamond a good thermal conductor?
2. Why do polymers tend to have high values of coefficient of thermal expansion?
3. Define the glass transition temperature.
4. Why does a thermal interface material need to be conformable?
5. What is the difference between a first-order phase transition and a second-order phase transition?
6. Why is the martensite phase of a shape memory alloy able to sustain a large reversible strain?
7. Describe the procedure for using a shape memory alloy as a temperature-sensitive actuator.
8. Describe a method of modifying a carbon fiber (continuous) epoxy-matrix composite in order to increase the through-thickness thermal conductivity.
9. Why are metal-matrix composites attractive for use in microelectric heat sinks?

## References

- [1] C.-K. Leong, Y. Aoyagi and D.D.L. Chung, "Carbon-Black Thixotropic Thermal Pastes for Improving Thermal Contacts", *J. Electron. Mater.* 34(10), 1336–1341 (2005).
- [2] C.-K. Leong, Y. Aoyagi and D.D.L. Chung, "Carbon Black Pastes as Coatings for Improving Thermal Gap-Filling Materials", *Carbon* 44(3), 435–440 (2006).
- [3] C.-K. Leong and D.D.L. Chung, "Carbon Black Dispersions as Thermal Pastes That Surpass Solder in Providing High Thermal Contact Conductance", *Carbon* 41(13), 2459–2469 (2003).
- [4] D.D.L. Chung, "Advances in Thermal Interface Materials", *Adv. Microelectron.* 33(4), 8–11 (2006).
- [5] Y. Xu, C.-K. Leong and D.D.L. Chung, "Carbon Nanotube Dispersions as Thermal Pastes", *J. Electron. Mater.* 36(9), 1181–1187 (2007).
- [6] H. Huang, C. Liu, Y. Wu and S. Fan, "Aligned Carbon Nanotube Composite Films for Thermal Management", *Adv. Mater.* 17, 1652–56 (2005).
- [7] T.A. Howe, C.-K. Leong and D.D.L. Chung, "Comparative Evaluation of Thermal Interface Materials for Improving the Thermal Contact Between an Operating Computer Microprocessor and its Heat Sink", *J. Electron. Mater.* 35(8):1628–1635 (2006).
- [8] C. Lin and D.D.L. Chung, "Graphite Nanoplatelet Pastes versus Carbon Black Pastes as Thermal Interface Materials", *Carbon* 47(1), 295–305 (2009).
- [9] C. Lin and D.D.L. Chung, "Effect of Carbon Black Structure on the Effectiveness of Carbon Black Thermal Interface Pastes", *Carbon* 45(15), 2922–31 (2007).
- [10] X. Fu and D.D.L. Chung, "Effect of Admixtures on the Thermal and Thermomechanical Behavior of Cement Paste", *ACI Mater. J.* 96(4), 455–461 (1999).

## Further Reading

- P.P.S.S. Abadi, C.-K. Leong and D.D.L. Chung, "Factors that Govern the Performance of Thermal Interface Materials", *J. Electron. Mater.* 38(1), 175–192 (2009).

- Y. Aoyagi and D.D.L. Chung, "Antioxidant-based phase-change thermal interface materials with high thermal stability", *J. Electron. Mater.* 37(4), 448–461 (2008).
- Y. Aoyagi, C.-K. Leong and D.D.L. Chung, "Polyol-Based Phase-Change Thermal Interface Materials", *J. Electron. Mater.* 35(3), 416–424 (2006).
- D.D.L. Chung, "Materials for Thermal Conduction", *Appl. Therm. Eng.* 21 (ER16), 1593–1605 (2001).
- D.D.L. Chung, "Cement-Matrix Composites for Thermal Engineering", *Appl. Therm. Eng.* 21(ER16), 1607–1619 (2001).
- D.D.L. Chung, "Advances in Thermal Interface Materials", *Adv. Microelectron.* 33(4), 8–11 (2006).
- D.D.L. Chung and C. Zweben, "Composites for Electronic Packaging and Thermal Management", *Comprehensive Composite Materials*, Pergamon, Oxford, 2000, vol. 6, pp. 701–725.
- Z. Liu and D.D.L. Chung, "Calorimetric Evaluation of Phase Change Materials for Use as Thermal Interface Materials", *Thermochim. Acta* 366(2), 135–147 (2001).
- Z. Liu and D.D.L. Chung, "Boron Nitride Particle Filled Paraffin Wax as a Phase-Change Thermal Interface Material", *J. Electron. Packag.* 128(4), 319–323 (2006).
- Z. Mei and D.D.L. Chung, "Thermoplastic Matrix Phase Transitions in a Carbon Fiber Composite, Studied by Contact Electrical Resistivity Measurement of the Interface between Two Unbonded Laminae", *Polym. Compos.* 23(5), 824–827 (2002).